

Supporting information

Competing forces in the self-assembly of amide-functionalized discotic mesogens

Jun Yoshida,^{a, b*} Kevin J. A. Bozek,^a John R. Thompson,^a and Vance E. Williams,^{a*}

^a Department of Chemistry, Simon Fraser University, 8888 University Drive, Burnaby, British Columbia, V6a 1S6, Canada.

^b Department of Chemistry, School of Science, Kitasato University, 1-15-1 Kitasato, Minamiku, Sagamihara, Kanagawa, 252-0329, Japan.

E-mail: vancew@sfu.ca

E-mail: yoshidaj@kitasato-u.ac.jp

Contents

| | |
|--|----|
| Materials and methods | 2 |
| General synthesis of dEt(n) and HBu(n) (n=6-12)..... | 3 |
| ¹ H NMR spectra of dEt(n) and HBu(n) (n = 6-12) | 6 |
| ¹³ C NMR spectra of dEt(n) and HBu(n) (n =6-12). | 14 |
| ESI-Mass spectra of dEt(n) and HBu(n) (n = 6-12)..... | 18 |
| ¹ H NMR spectra of HBu(8) in the presence of triethylamine. | 26 |
| 2D NMR spectroscopy and peak assignments..... | 27 |
| ¹ H NMR dilution experiments and analysis | 34 |
| Single crystal X-ray diffraction study..... | 41 |
| DSC data..... | 42 |
| POM photographs..... | 48 |
| X-ray diffraction patterns | 49 |
| References..... | 51 |

Materials and methods

All solvents employed were reagent grade. Diethylamine, butylamine, and oxalyl chloride were purchased from Aldrich and used without further purification. Dibenzophenazine carboxylic acids were prepared according to a literature procedure.^{1,2} ¹H NMR were measured at 400 MHz or 500 MHz (Bruker Avance III 400 or 500 spectrometer) and ¹³C NMR were measured at 126 MHz. 2D NMR spectroscopy (HMBC, HSQC, COSY) was also performed for **HBu(n)** and **dEt(n)** (n=6-12). Infrared spectroscopy in ATR mode was carried out on a UATR TWO (Perkin Elmer) spectrometer. High resolution mass spectrometry was carried out on a Bruker micrOTOF (ESI⁺) using an acetonitrile as the solvent.

Texture analysis was carried out using optical polarizing microscopy on an Olympus BX50 microscope with crossed polarizers using a Linkam LTS350 heating stage. Phase transition temperatures and enthalpies were investigated using differential scanning calorimetry (DSC) on a Perkin Elmer DSC, heating and cooling at a rate of 10 °C min⁻¹. X-ray diffraction studies of liquid crystalline samples were carried out on a Rigaku RAXIS rapid diffractometer using Cu K α radiation, a graphite monochromator and a Fujifilm Co., Ltd curved image plate (460 mm x 256 mm). A 0.1 mm collimator was used and typical irradiation times were of 30 minutes. A home made capillary furnace was used for variable temperature measurements.³

Dynamic light scattering (DLS) experiments were conducted on a Zetasizer Nano ZS ZEN 3600 by Malvern Instruments equipped with a red laser (633 nm). Hydrodynamic diameter measurements of all **dEt(n)** and **HBu(n)** series in chloroform (viscosity: 0.05370 cP, refractive index: 1.44) were carried out by dynamic light scattering. All measurements were performed at 25 °C in a glass cuvette. Sample volumes were set to 1 mL. Prepared solutions (10 – 70 mM) were filtered through 0.2 μ m Acrodisc CR 13 mm syringe filters with PTFE membranes (Life Sciences). 10-20 scans are performed for each measurement. The equipment determines the scan number automatically. For each compound at each concentration, 5 measurements were performed and averaged. The results of DLS were analyzed as an intensity size distribution (results were not converted to a volume or number size distribution). Two peaks were often observed in the intensity size distribution, since the observed intensity I is proportional to the sixth power of the particle diameter d ($I \propto d^6$). Even an extremely small number of large particles (trace impurities) can result in a large peak in the intensity size distribution. Because of this, only the peak corresponding to a smaller particle size (10 to 30 Å) was considered.

General synthesis of **dEt(n)** and **HBu(n)** (n=6-12)

To a flame-dried flask, dry dichloromethane (50 ml), 2,3,6,7-tetrakis(alkoxy)dibenzo[a,c]phenazine-11-carboxylic acid (500 mg), N,N'-dimethylformamide (1.0 eq.), and oxalylchloride (1.3 eq.) were successively added. The mixture was heated to 40 °C and stirred for 3 h. After the solvent was removed in vacuo, the solid were dispersed in dichloromethane (50 ml). To this dispersion, an excess amine (1.0~2.0 ml) was added. After the mixture was stirred for additional 1 h, it was extracted by dichloromethane. The combined organic extracts were dried over Na₂SO₄ and concentrated under reduced pressure. The crude was subjected to silica gel column chromatography (solvent: dichloromethane~dichloromethane/ethylacetate = 20/1).

N,N-diethyl-2,3,6,7-tetrakis(hexyloxy)dibenzo[a,c]phenazine-11-carboxamide (**dEt(6)**), a yellow solid (41% yield); ¹H NMR (400 MHz, CDCl₃, 54 mM) δ 8.76 (s, 1H), 8.72 (s, 1H), 8.32 (d, *J* = 8.6 Hz, 1H), 8.27 (d, *J* = 1.7 Hz, 1H), 7.79 (dd, *J* = 8.6, 1.8 Hz, 1H), 7.69 (d, *J* = 5.3 Hz, 2H), 4.34 (q, *J* = 6.5 Hz, 4H), 4.28 (td, *J* = 6.5, 2.0 Hz, 4H), 3.66 (s, 2H), 3.41 (s, 2H), 2.05 - 1.90 (m, 8H), 1.67 - 1.54 (m, 8H), 1.50 - 1.12 (m, 22H), 0.95 (t, *J* = 7.0 Hz, 12H).

¹³C NMR (126 MHz, CDCl₃, 54 mM) δ 170.58, 152.12, 152.06, 149.54, 142.63, 142.57, 141.49, 140.94, 137.49, 129.81, 127.37, 126.89, 126.81, 123.71, 123.63, 108.91, 108.86, 106.46, 69.71, 69.28, 69.25, 31.82, 29.46, 29.40, 25.99, 25.96, 22.81, 22.79, 14.21, 14.19.

HRMS (ESI⁺): calculated for C₄₉H₇₀N₃O₅ 780.5310, found 780.5331.

N,N-diethyl -2,3,6,7-tetrakis(octyloxy)dibenzo[a,c]phenazine-11-carboxamide (**dEt(8)**), a yellow solid (80% yield);

¹H NMR (400 MHz, CDCl₃, 56 mM) δ 8.76 (s, 1H), 8.71 (s, 1H), 8.32 (d, *J* = 8.7 Hz, 1H), 8.27 (d, *J* = 1.6 Hz, 1H), 7.79 (dd, *J* = 8.6, 1.8 Hz, 1H), 7.69 (d, *J* = 5.3 Hz, 2H), 4.33 (q, *J* = 6.5 Hz, 4H), 4.27 (td, *J* = 6.5, 2.1 Hz, 4H), 3.66 (s, 2H), 3.41 (s, 2H), 2.05 - 1.90 (m, 8H), 1.67 - 1.52 (m, 8H), 1.51 - 1.10 (m, 38H), 0.90 (t, *J* = 6.8 Hz, 12H).

¹³C NMR (126 MHz, CDCl₃, 56 mM) δ 170.58, 152.12, 152.07, 149.54, 142.63, 142.56, 141.48, 140.93, 137.48, 129.80, 127.37, 126.89, 126.79, 123.70, 123.63, 108.93, 108.87, 106.48, 69.72, 69.29, 69.27, 32.01, 32.00, 29.62, 29.52, 29.49, 29.48, 29.46, 26.34, 26.33, 26.31, 22.85, 22.84, 14.27, 14.26.

HRMS (ESI⁺): calculated for C₅₇H₈₆N₃O₅ 892.6562, found 892.6575.

N,N-diethyl -2,3,6,7-tetrakis(decyloxy)dibenzo[*a,c*]phenazine-11-carboxamide

(**dEt(10)**), a yellow solid (42% yield);

¹H NMR (400 MHz, CDCl₃, 44 mM) δ 8.76 (s, 1H), 8.72 (s, 1H), 8.32 (d, *J* = 8.8 Hz, 1H), 8.28 (d, *J* = 1.5 Hz, 1H), 7.79 (dd, *J* = 8.6, 1.8 Hz, 1H), 7.70 (d, *J* = 4.4 Hz, 2H), 4.33 (q, *J* = 6.5 Hz, 4H), 4.28 (td, *J* = 6.5, 1.8 Hz, 4H), 3.66 (s, 2H), 3.41 (s, 2H), 2.06 – 1.88 (m, 8H), 1.72 – 1.52 (m, 8H), 1.52 – 1.09 (m, 54H), 0.89 (t, *J* = 6.8 Hz, 12H).

¹³C NMR (126 MHz, CDCl₃, 44 mM) δ 170.59, 152.13, 152.08, 149.56, 142.64, 142.58, 141.49, 140.94, 137.49, 129.81, 127.38, 126.90, 126.81, 123.71, 123.65, 108.95, 108.89, 106.50, 69.74, 69.30, 69.28, 32.08, 29.85, 29.77, 29.68, 29.66, 29.54, 29.46, 26.32, 22.85, 14.27.

HRMS (ESI⁺): calculated for C₆₅H₁₀₂N₃O₅ 1004.7814, found 1004.7825.

N,N-diethyl -2,3,6,7-tetrakis(dodecyloxy)dibenzo[*a,c*]phenazine-11-carboxamide

(**dEt(12)**), a yellow solid (62% yield);

¹H NMR (400 MHz, CDCl₃, 45 mM) δ 8.76 (s, 1H), 8.73 (s, 1H), 8.32 (d, *J* = 8.7 Hz, 1H), 8.28 (d, *J* = 1.7 Hz, 1H), 7.79 (dd, *J* = 8.6, 1.8 Hz, 1H), 7.70 (d, *J* = 4.0 Hz, 2H), 4.33 (q, *J* = 6.5 Hz, 4H), 4.28 (td, *J* = 6.4, 1.6 Hz, 4H), 3.66 (s, 2H), 3.41 (s, 2H), 2.06 – 1.90 (m, 8H), 1.66 – 1.53 (m, 8H), 1.53 – 1.10 (m, 70H), 0.88 (t, *J* = 6.8 Hz, 12H).

¹³C NMR (126 MHz, CDCl₃, 45 mM) δ 170.57, 151.97, 151.92, 149.38, 142.55, 142.49, 141.39, 140.85, 137.37, 129.79, 127.33, 126.80, 126.70, 123.55, 123.46, 108.63, 108.57, 106.15, 77.41, 77.16, 76.91, 69.57, 69.18, 69.15, 32.08, 29.90, 29.84, 29.69, 29.67, 29.55, 29.46, 29.41, 26.33, 26.30, 22.85, 14.30.

HRMS (ESI⁺): calculated for C₇₃H₁₁₈N₃O₅ 1116.9066, found 1116.9044.

N-butyl-2,3,6,7-tetrakis(hexyloxy)dibenzo[*a,c*]phenazine-11-carboxamide (**HBu(6)**), a yellow solid (57% yield);

¹H NMR (400 MHz, CDCl₃, 13 mM) δ 8.71 (d, *J* = 4.0 Hz, 2H), 8.58 (d, *J* = 1.7 Hz, 1H), 8.33 (d, *J* = 8.8 Hz, 1H), 8.21 (dd, *J* = 8.8, 1.9 Hz, 1H), 7.66 (s, 1H), 7.65 (s, 1H), 6.50 (t, *J* = 5.6 Hz, 1H), 4.40 – 4.19 (m, 8H), 3.59 (q, *J* = 6.7 Hz, 2H), 2.04 – 1.91 (m, 8H), 1.77 – 1.55 (m, 10H), 1.55 – 1.33 (m, 18H), 1.02 (t, *J* = 7.3 Hz, 3H), 0.99 – 0.88 (m, 12H).

¹³C NMR (126 MHz, CDCl₃, 73 mM) δ 167.66, 151.91, 151.70, 149.28, 149.13, 142.48, 142.34, 142.20, 140.35, 135.01, 129.48, 127.53, 127.15, 126.60, 126.41, 123.29, 123.13, 108.47, 108.42, 106.03, 105.78, 69.56, 69.42, 69.12, 69.03, 40.31, 32.02, 31.89, 31.87, 29.54, 29.51, 29.47, 26.06, 26.03, 26.02, 25.99, 22.84, 22.82, 20.46, 14.23, 14.21, 14.02.

HRMS (ESI⁺): calculated for C₄₉H₇₀N₃O₅ 780.5310, found 780.5303.

N-butyl-2,3,6,7-tetrakis(octyloxy)dibenzo[*a,c*]phenazine-11-carboxamide (**HBu(8)**), a yellow solid (62% yield);

¹H NMR (400 MHz, CDCl₃, 49 mM) δ 8.41 (s, 2H), 8.36 (s, 1H), 8.14 (d, *J* = 8.7 Hz, 1H), 8.11 (dd, *J* = 8.8, 1.6 Hz, 1H), 7.43 (s, 1H), 7.36 (s, 1H), 6.76 (t, *J* = 5.6 Hz, 1H), 4.32 – 4.10 (m, 8H), 3.59 (q, *J* = 6.7 Hz, 2H), 2.07 – 1.88 (m, 8H), 1.82 – 1.68 (m, 2H), 1.67 – 1.26 (m, 42H), 1.04 (t, *J* = 7.4 Hz, 3H), 0.92 (d, *J* = 6.8 Hz, 12H).

¹³C NMR (126 MHz, CDCl₃, 49 mM) δ 167.61, 151.97, 151.76, 149.33, 149.19, 142.52, 142.36, 142.24, 140.37, 135.04, 129.50, 127.52, 127.20, 126.66, 126.47, 123.32, 123.17, 108.55, 108.49, 106.12, 105.87, 32.06, 32.03, 29.72, 29.70, 29.59, 29.54, 26.42, 26.38, 26.35, 22.88, 22.86, 20.46, 14.28, 14.27, 14.02.

HRMS (ESI⁺): calculated for C₅₇H₈₆N₃O₅ 892.6562, found 892.6596.

N-butyl-2,3,6,7-tetrakis(decyloxy)dibenzo[*a,c*]phenazine-11-carboxamide (**HBu(10)**), a yellow solid (53% yield);

¹H NMR (500 MHz, CDCl₃, 35 mM) δ 8.58 (d, *J* = 2.8 Hz, 2H), 8.48 (d, *J* = 1.6 Hz, 1H), 8.25 (d, *J* = 8.8 Hz, 1H), 8.17 (dd, *J* = 8.8, 1.8 Hz, 1H), 7.56 (s, 1H), 7.52 (s, 1H), 6.61 (t, *J* = 5.6 Hz, 1H), 4.32 – 4.17 (m, 8H), 3.59 (q, *J* = 6.7 Hz, 2H), 2.05 – 1.89 (m, 8H), 1.73 (dt, *J* = 14.9, 7.4 Hz, 2H), 1.65 – 1.55 (m, 8H), 1.55 – 1.20 (m, 50H), 1.03 (t, *J* = 7.4 Hz, 3H), 0.89 (t, *J* = 6.7 Hz, 12H).

¹³C NMR (126 MHz, CDCl₃, 35 mM) δ 167.68, 151.89, 151.67, 149.27, 149.11, 142.43, 142.32, 142.16, 140.33, 135.01, 129.46, 127.53, 127.13, 126.57, 126.38, 123.28, 123.11, 108.46, 108.41, 106.05, 105.75, 69.58, 69.41, 69.12, 69.02, 40.31, 32.11, 32.04, 29.92, 29.84, 29.80, 29.77, 29.63, 29.62, 29.58, 26.44, 26.40, 26.37, 22.86, 20.47, 14.26, 14.03.

HRMS (ESI⁺): calculated for C₆₅H₁₀₂N₃O₅ 1004.7814, found 1004.7834.

N-butyl-2,3,6,7-tetrakis(dodecyloxy)dibenzo[*a,c*]phenazine-11-carboxamide (**HBu(12)**), a yellow solid (71% yield);

¹H NMR (400 MHz, CDCl₃, 19 mM) δ 8.58 (d, *J* = 4.3 Hz, 2H), 8.49 (s, 1H), 8.25 (d, *J* = 8.8 Hz, 1H), 8.17 (dd, *J* = 8.8, 1.8 Hz, 1H), 7.56 (s, 1H), 7.52 (s, 1H), 6.63 (t, *J* = 5.6 Hz, 1H), 4.25 (ddt, *J* = 17.9, 13.1, 6.5 Hz, 8H), 3.59 (q, *J* = 6.7 Hz, 2H), 2.05 – 1.90 (m, 8H), 1.73 (dd, *J* = 8.4, 6.1 Hz, 2H), 1.67 – 1.20 (m, 74H), 1.03 (t, *J* = 7.3 Hz, 3H), 0.88 (t, *J* = 6.8 Hz, 12H).

¹³C NMR (126 MHz, CDCl₃, 116 mM) δ 167.81, 151.76, 151.52, 149.14, 148.94, 142.16, 142.06, 141.86, 140.09, 135.01, 129.26, 127.47, 127.06, 126.41, 126.21, 123.06, 122.85, 108.28, 105.87, 105.50, 69.49, 69.29, 69.04, 68.92, 40.33, 32.10, 32.06, 29.96, 29.94,

29.93, 29.91, 29.88, 29.85, 29.82, 29.65, 29.56, 26.47, 26.43, 26.39, 22.85, 20.49, 14.25, 14.04.

HRMS (ESI⁺): calculated for C₇₃H₁₁₈N₃O₅ 1116.9066, found 1116.9035.

¹H NMR spectra of **dEt(n)** and **HBu(n)** (n = 6-12)

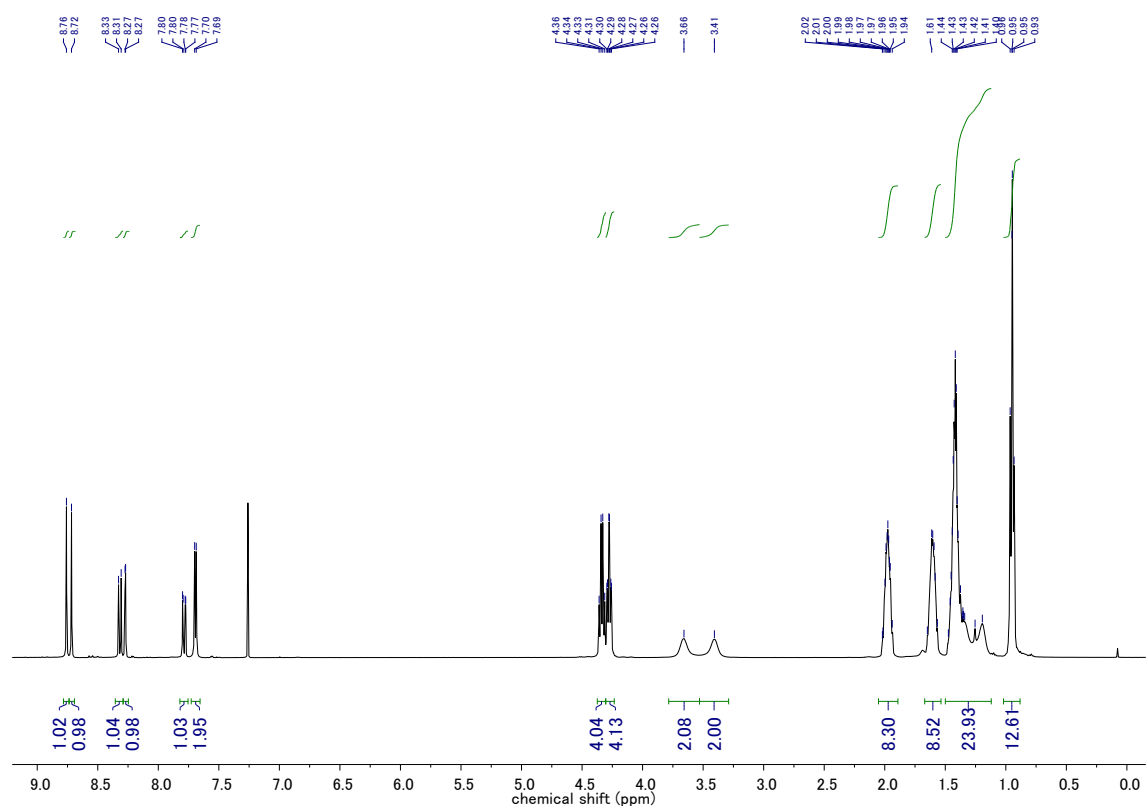


Figure S1. ¹H NMR spectrum of **dEt(6)** measured at 54 mM in CDCl₃.

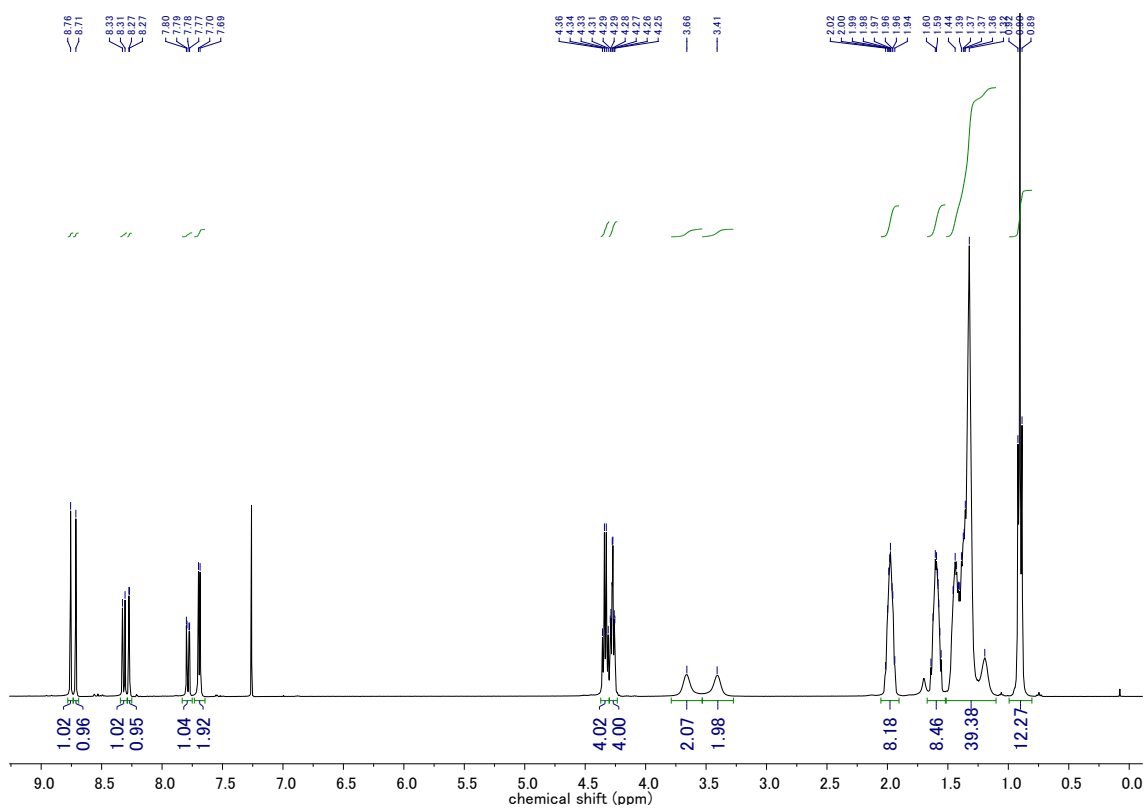


Figure S2. ^1H NMR spectrum of **dEt(8)** measured at 56 mM in CDCl_3 .

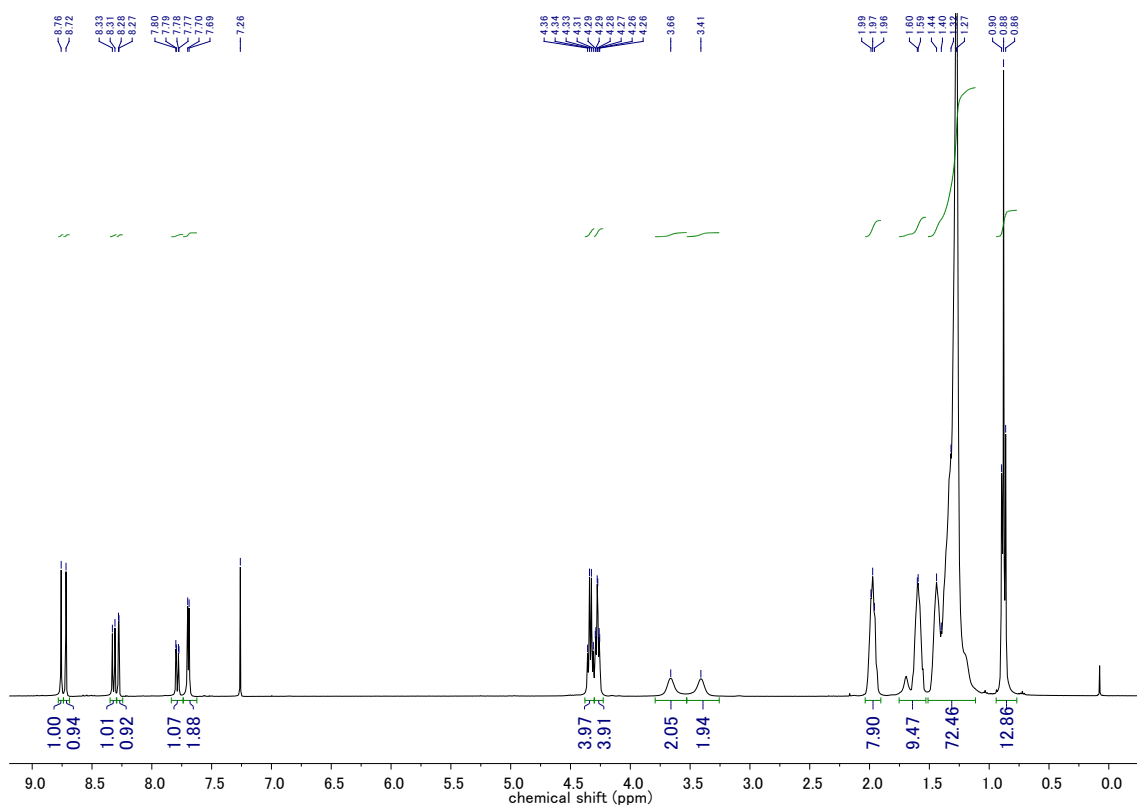


Figure S4. ¹H NMR spectrum of dEt(12) measured at 45 mM in CDCl₃.

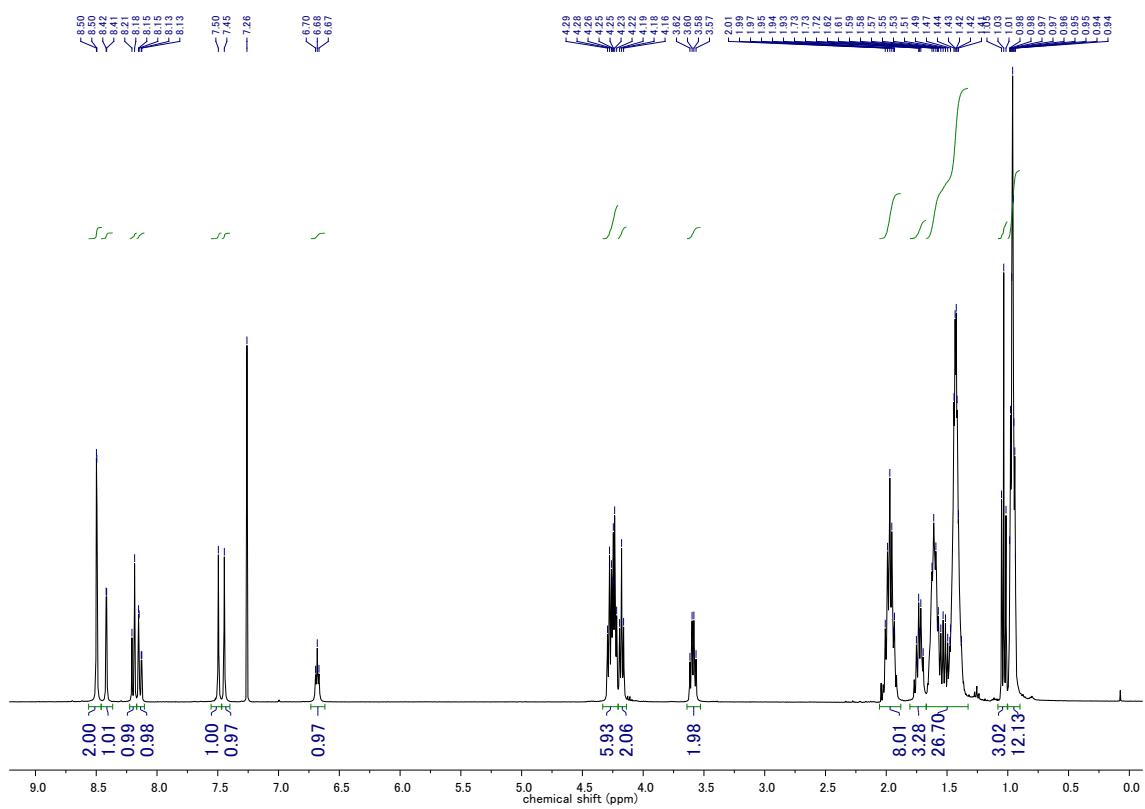


Figure S5. ^1H NMR spectrum of **HBu(6)** measured at 48 mM in CDCl_3 .

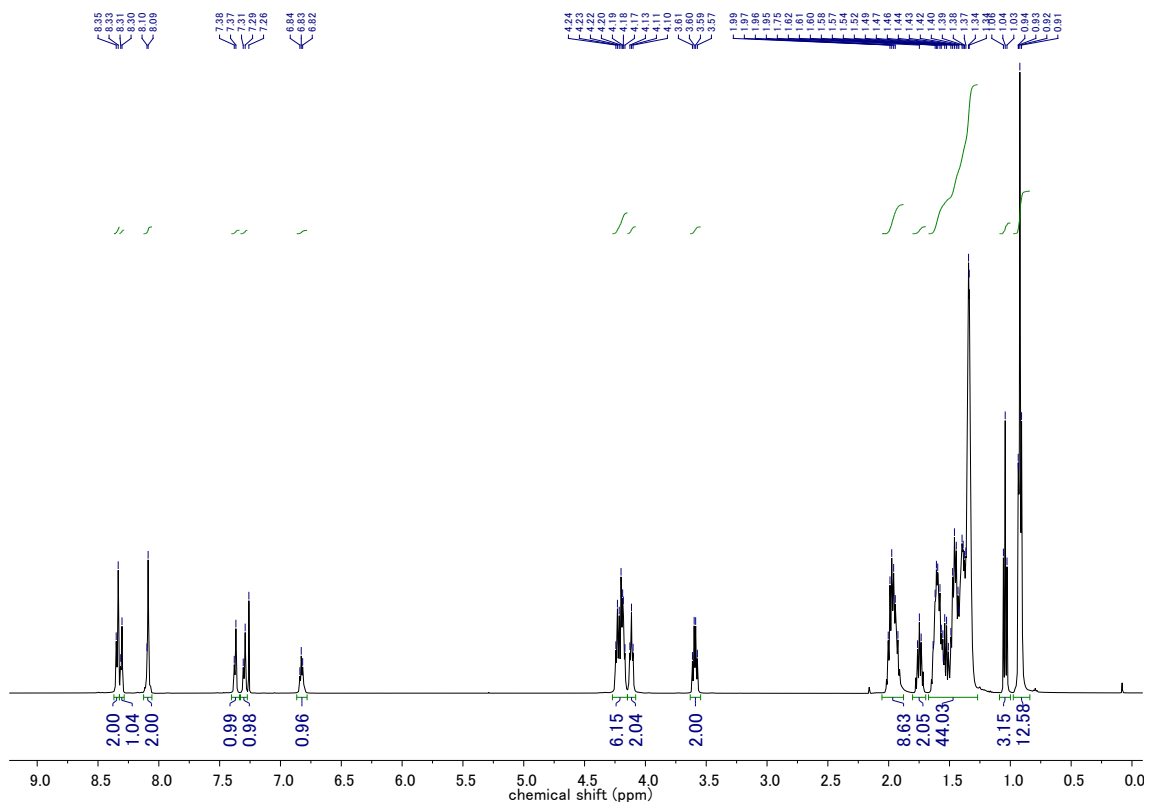


Figure S6. ^1H NMR spectrum of **HBU(8)** measured at 73 mM in CDCl_3 .

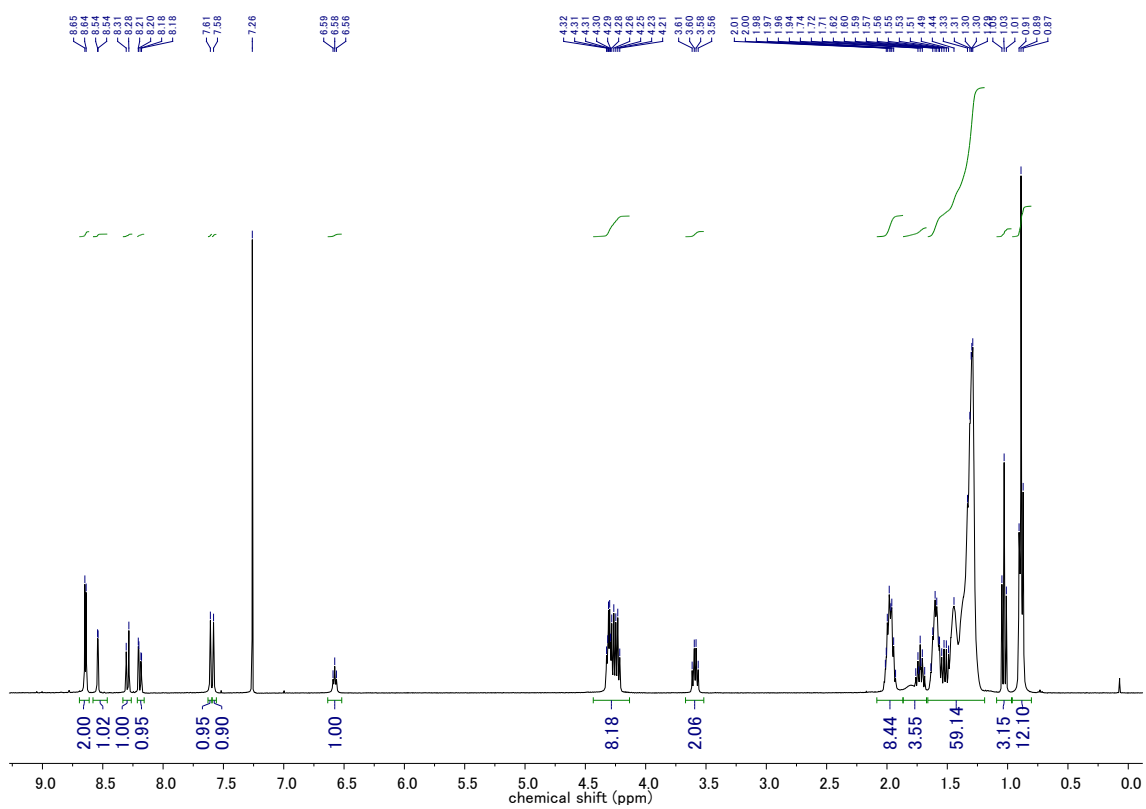


Figure S7. ^1H NMR spectrum of **HBU(10)** measured at 9.6 mM in CDCl_3 .

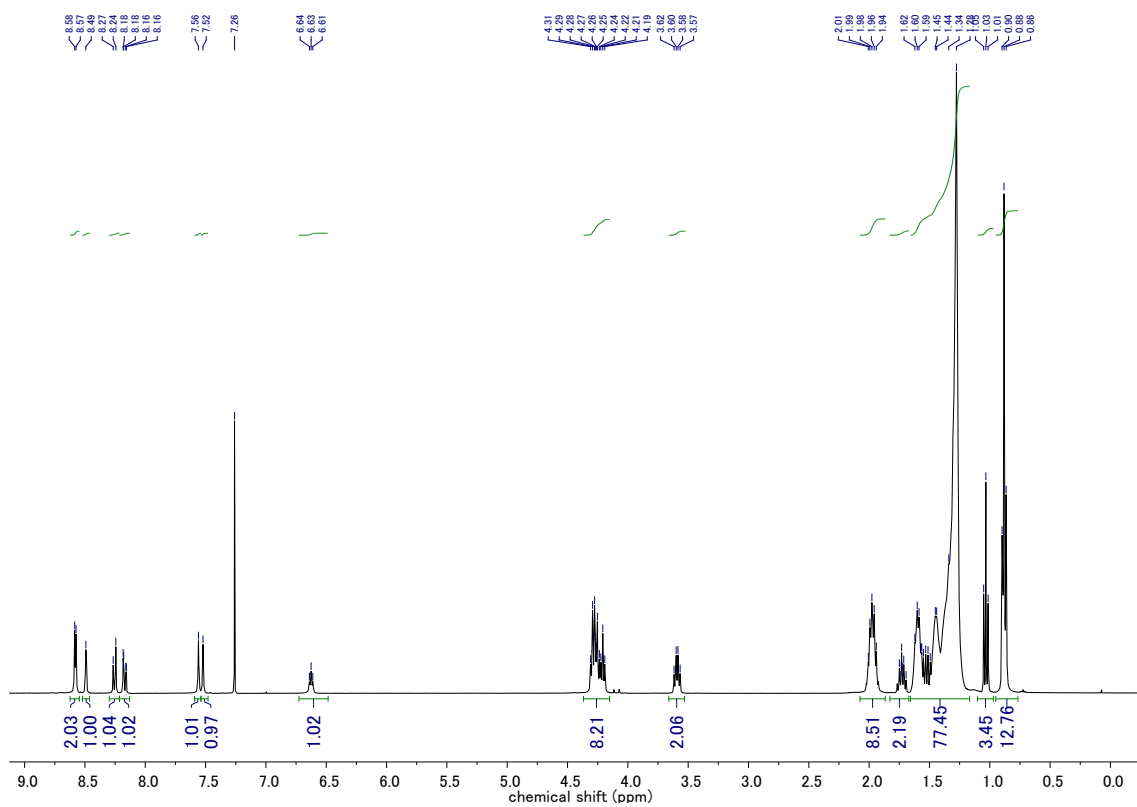


Figure S8. ^1H NMR spectrum of **HBU(12)** measured at 19 mM in CDCl_3 .

^{13}C NMR spectra of **dEt(n)** and **HBu(n)** ($n = 6-12$).

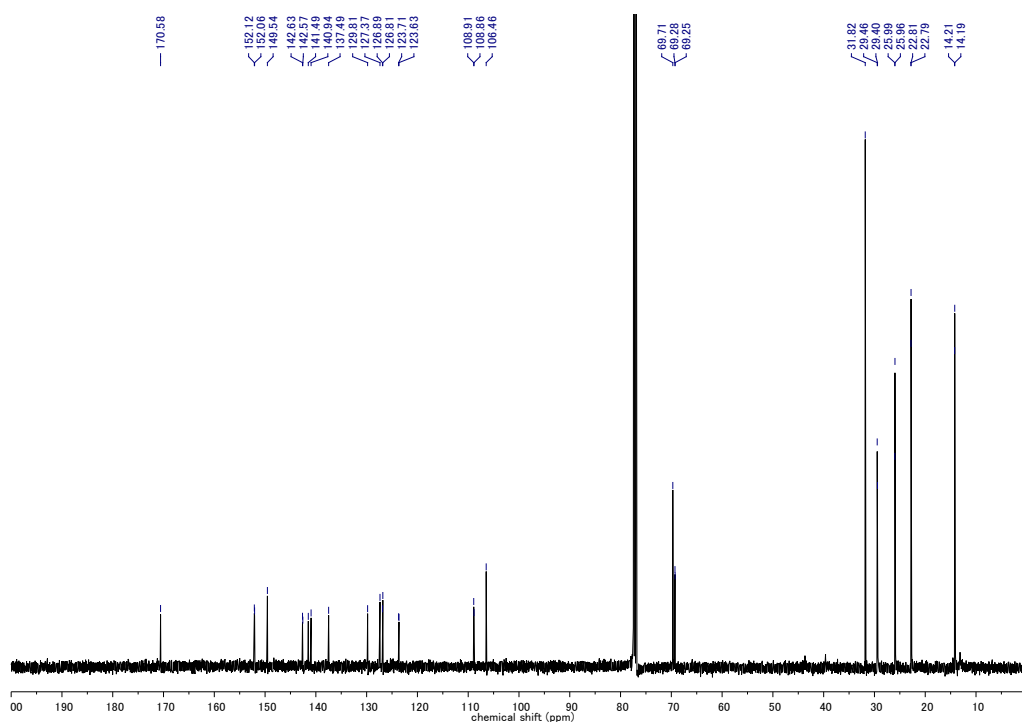


Figure S9. ^{13}C NMR spectrum of **dEt(6)** measured at 54 mM in CDCl_3 .

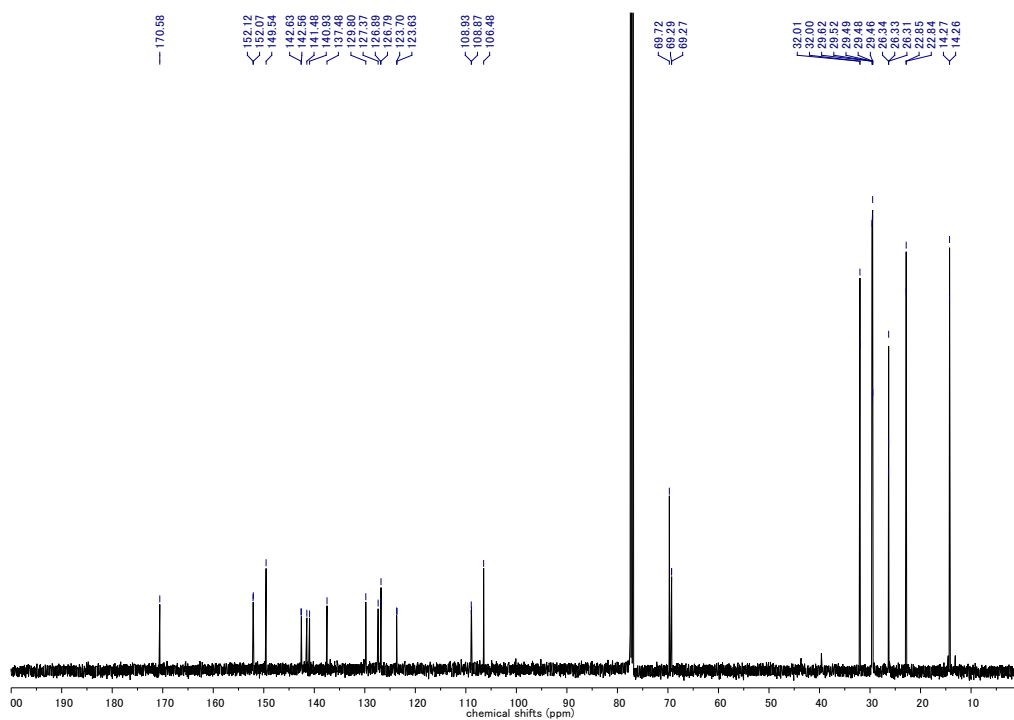


Figure S10. ^{13}C NMR spectrum of **dEt(8)** measured at 56 mM in CDCl_3 .

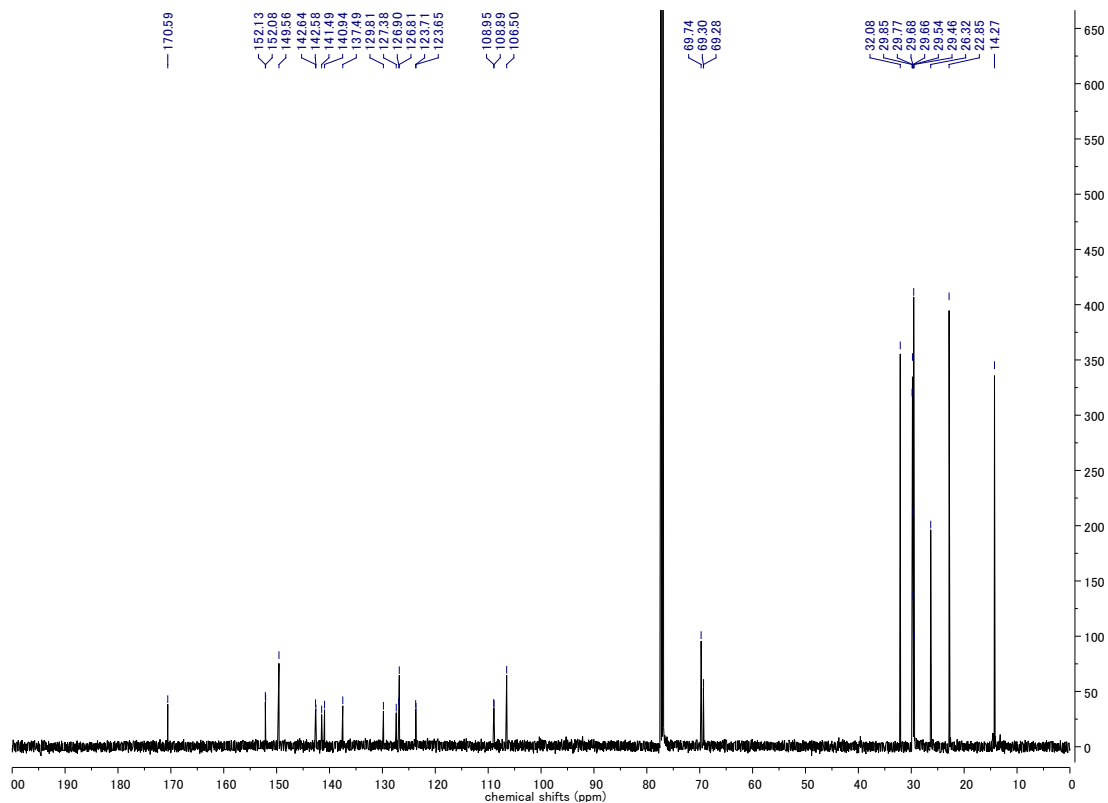


Figure S11. ^{13}C NMR spectrum of **dEt(10)** measured at 44 mM in CDCl_3 .

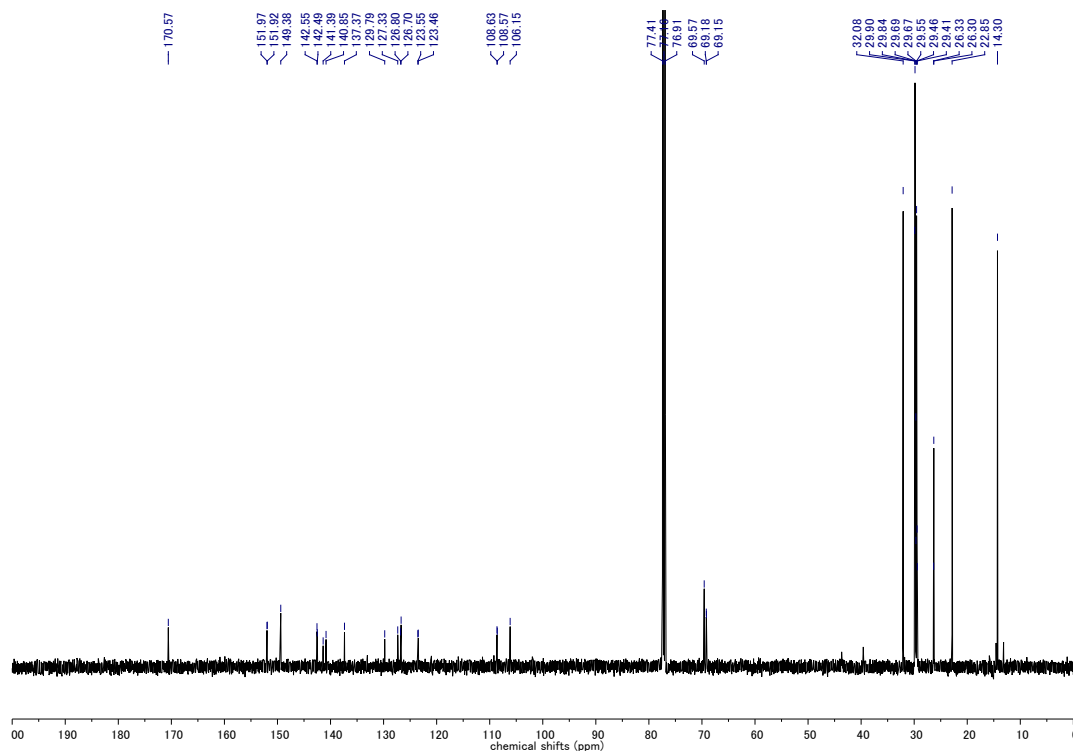


Figure S12. ^{13}C NMR spectrum of **dEt(12)** measured at 45 mM in CDCl_3 .

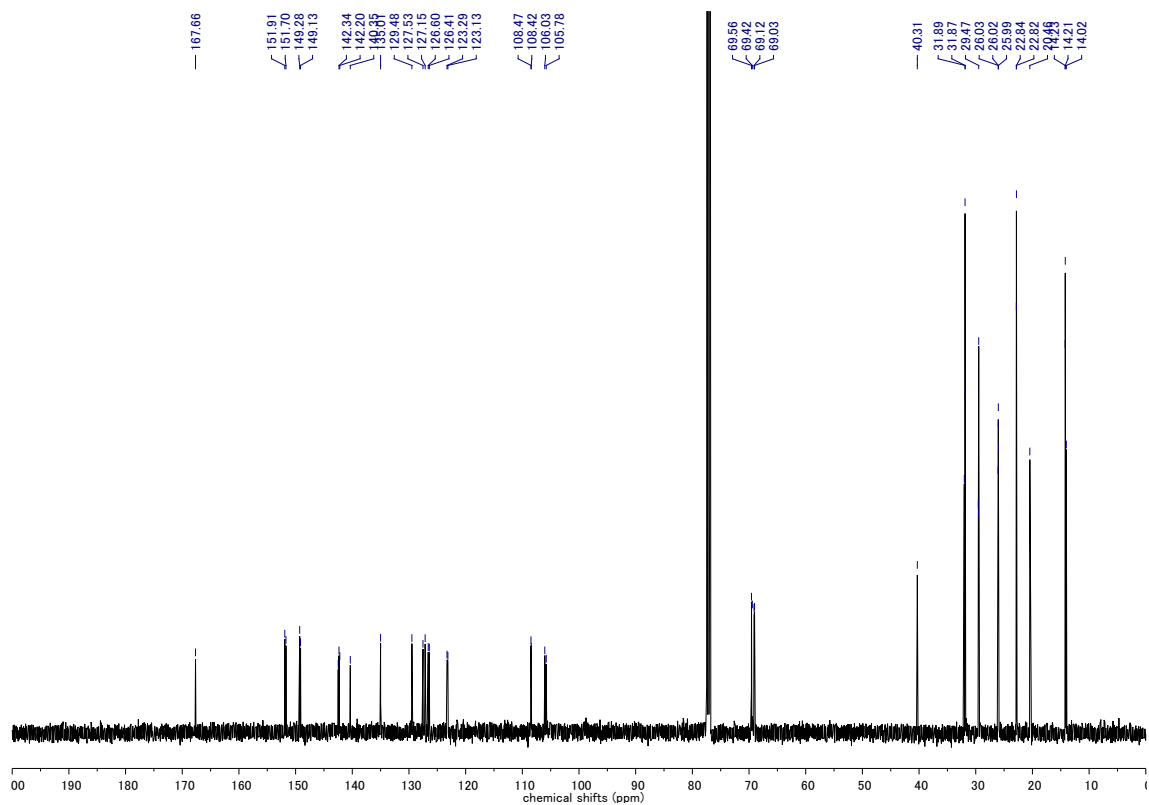


Figure S13. ^{13}C NMR spectrum of **HBU(6)** measured at 73 mM in CDCl_3 .

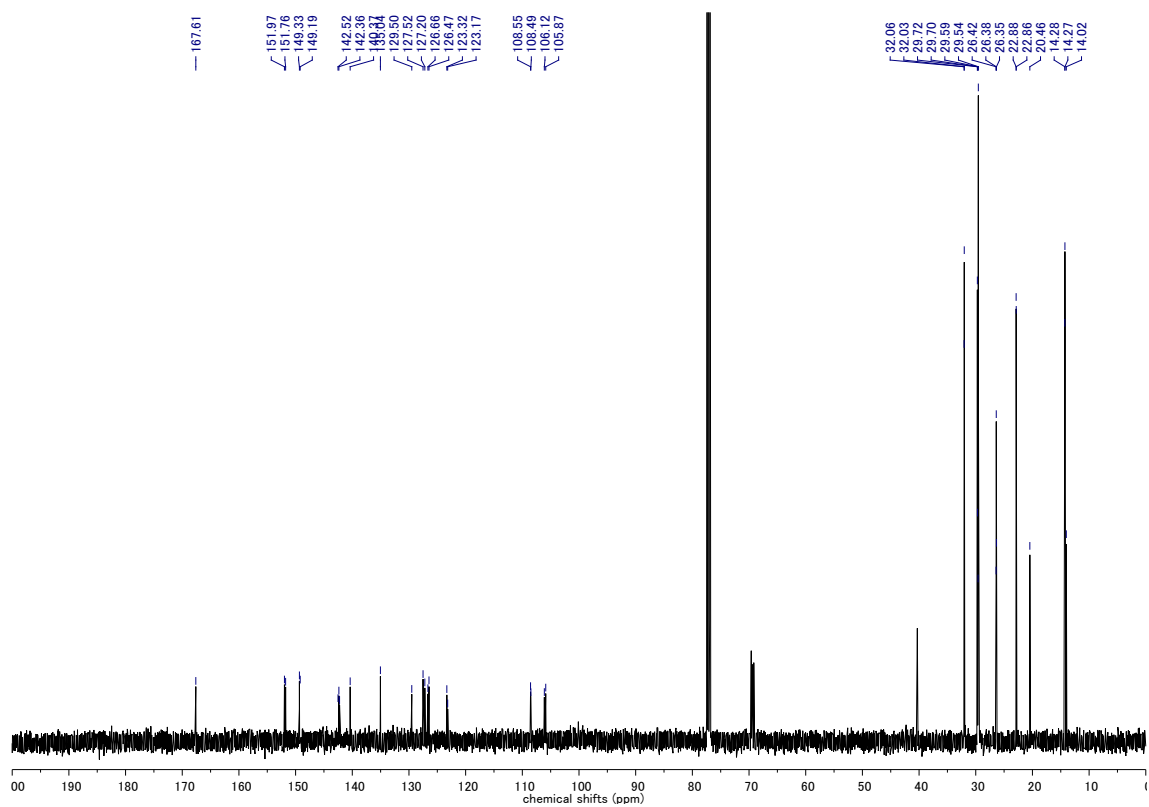


Figure S14. ^{13}C NMR spectrum of **HBU(8)** measured at 49 mM in CDCl_3 .

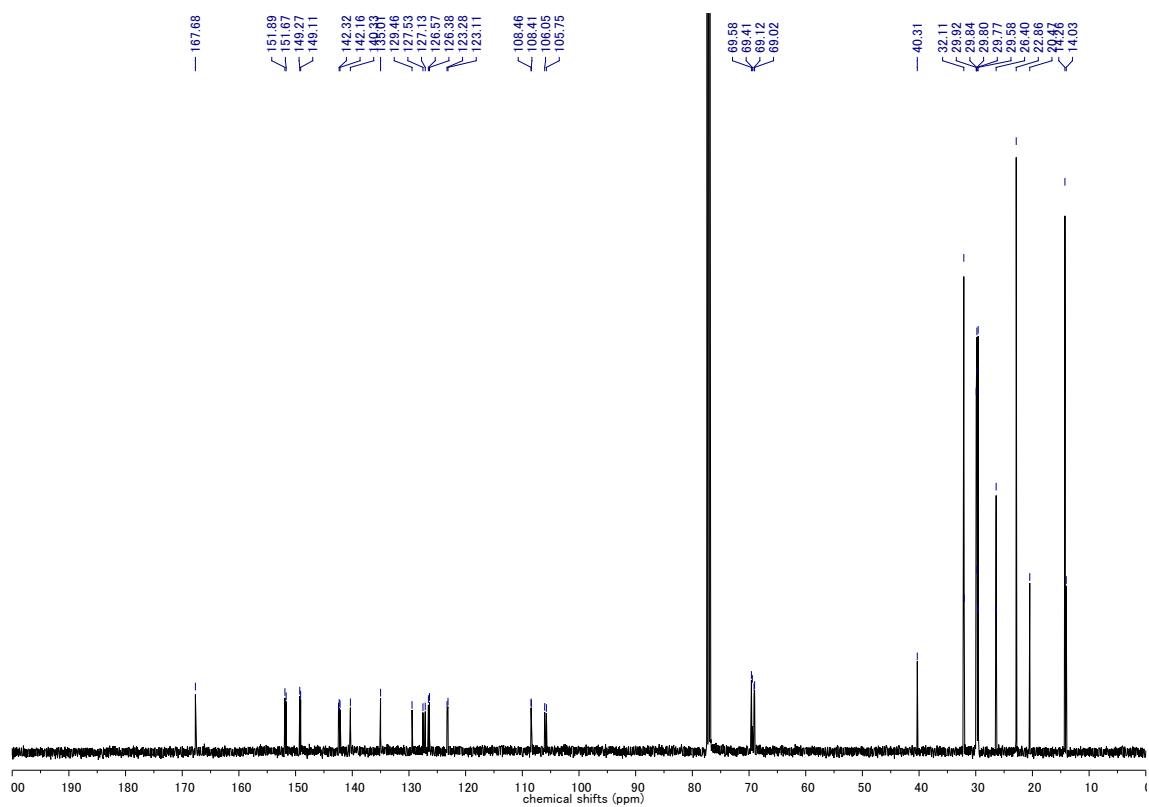


Figure S15. ^{13}C NMR spectrum of **HBu(10)** measured at 53 mM in CDCl_3 .

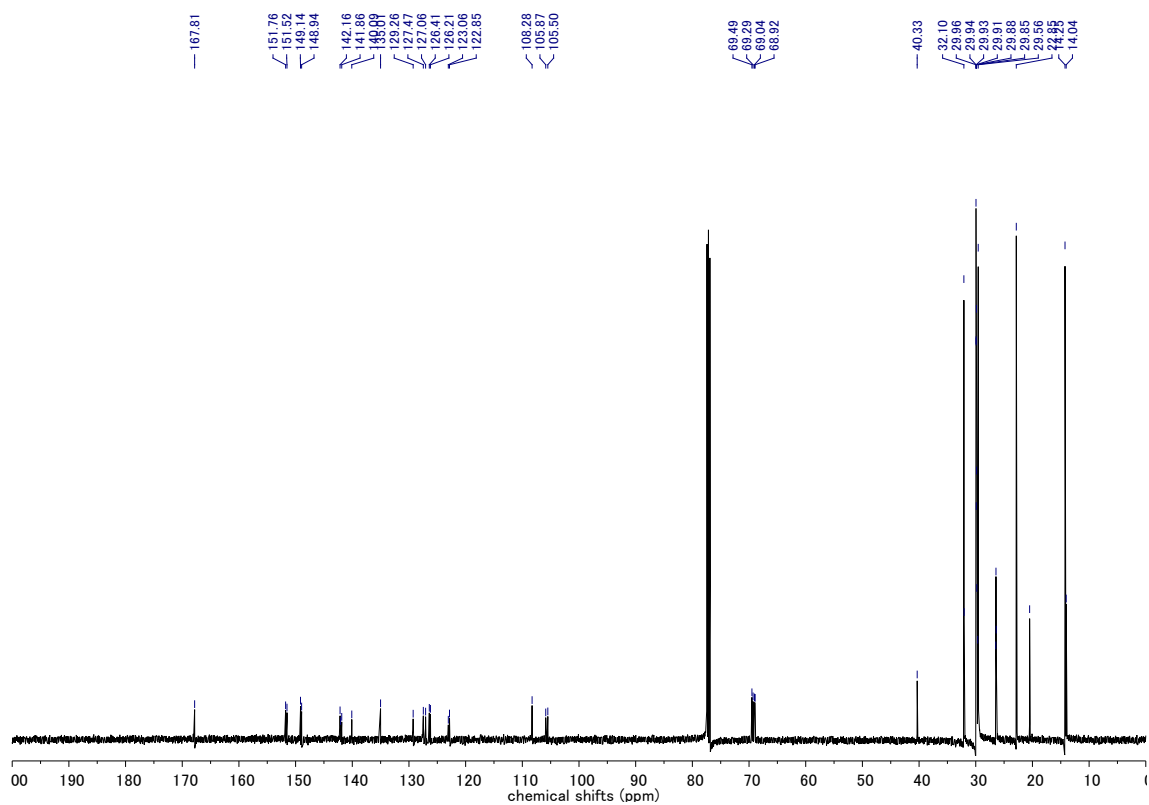


Figure S16. ^{13}C NMR spectrum of **HBu(12)** measured at 116 mM in CDCl_3 .

ESI-Mass spectra of **dEt(n)** and **HBu(n)** (n = 6-12)

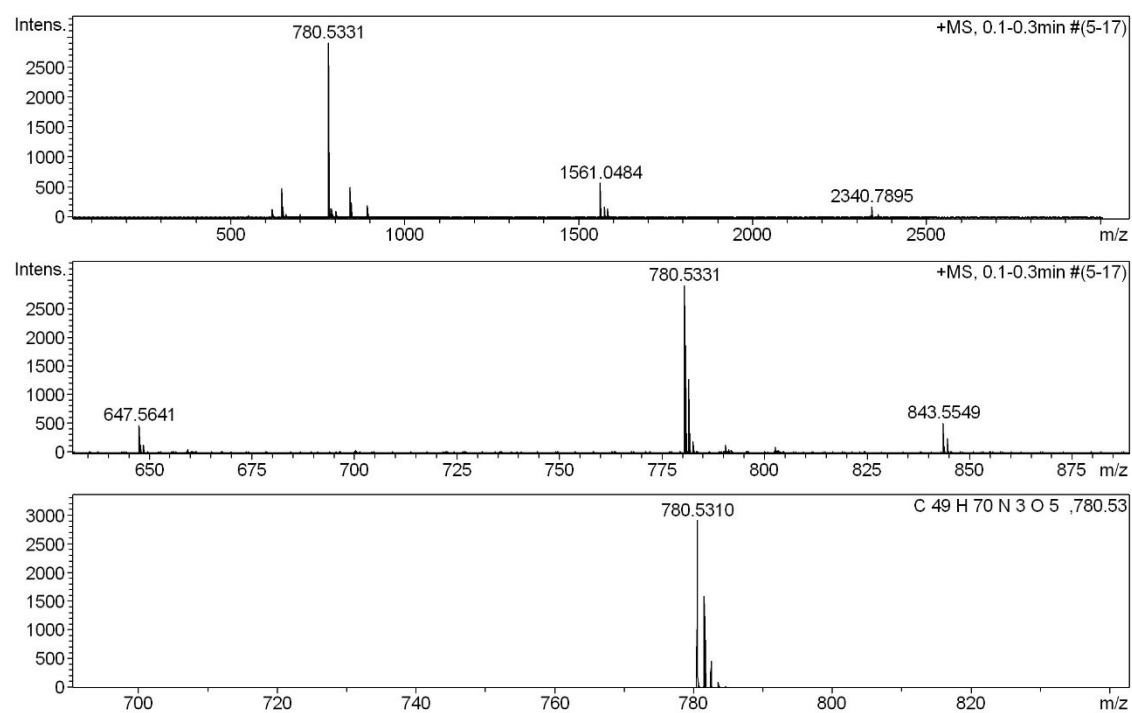


Figure S17. Experimental isotopic patterns of **dEt(6)** (Top two patterns) and theoretical isotopic pattern (bottom) for $[C_{49}H_{70}N_3O_5]^+$ (**dEt(6)** + H^+) in the ESI-MS measurement.

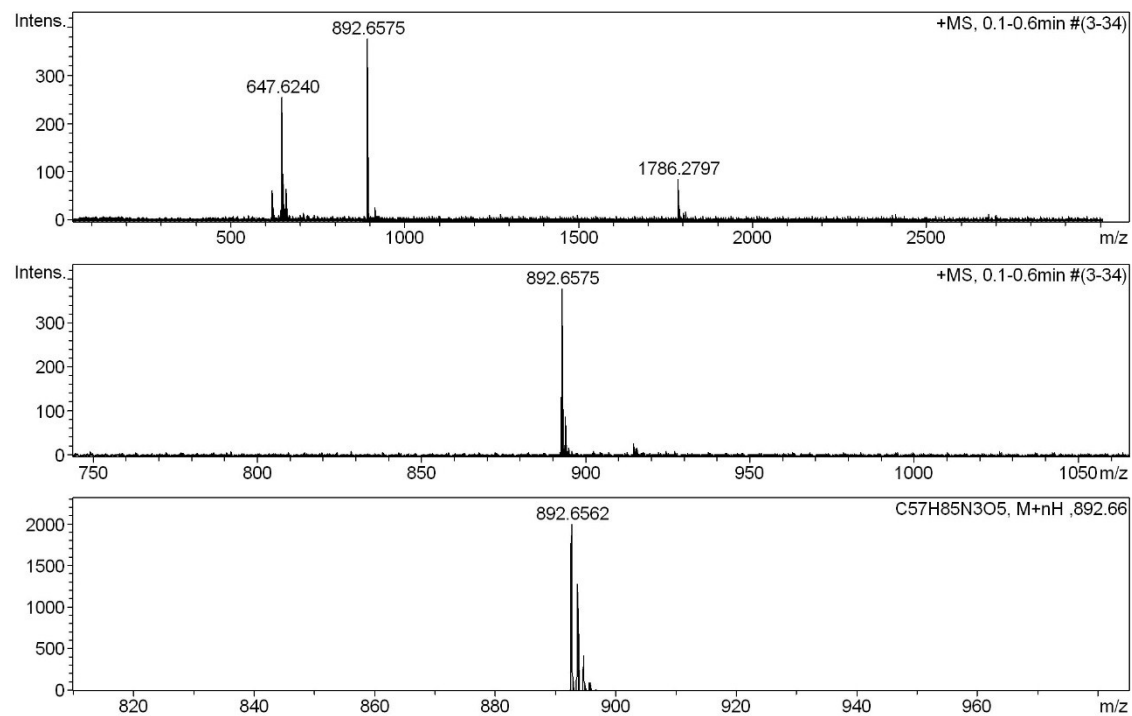


Figure S18. Experimental isotopic patterns of **dEt(8)** (Top two patterns) and theoretical isotopic pattern (bottom) for $[C_{57}H_{86}N_3O_5]^+$ ($[dEt(8) + H]^+$) in the ESI-MS measurement.

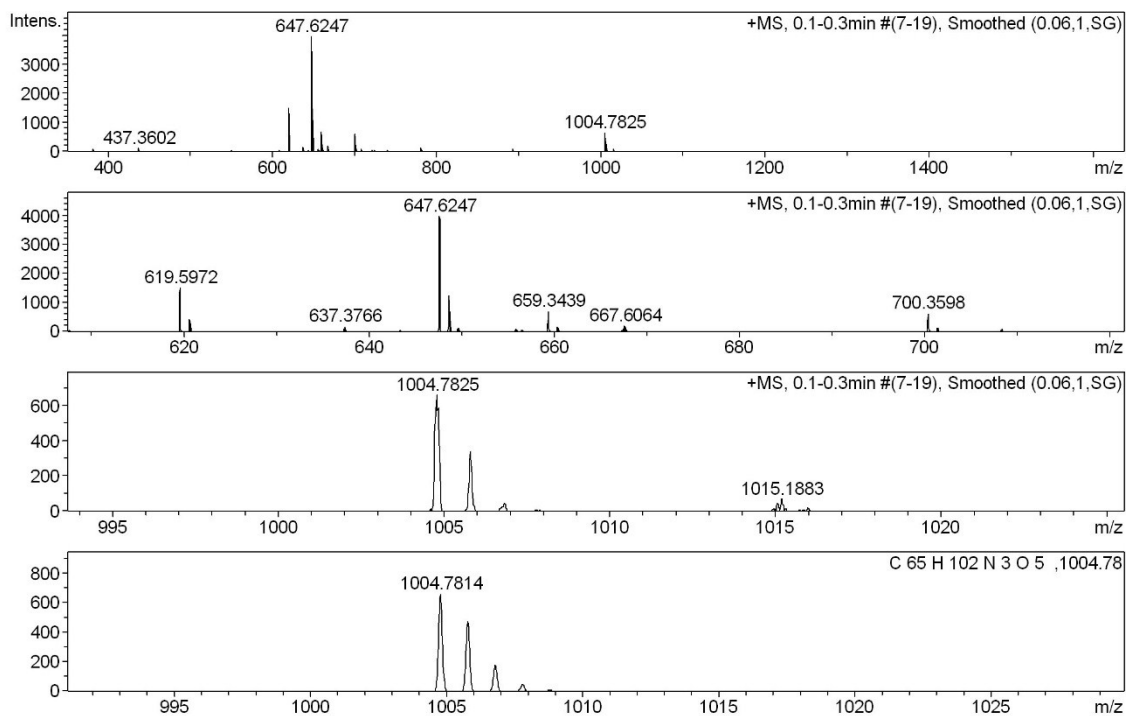


Figure S19. Experimental isotopic patterns of **dEt(10)** (top three patterns) and theoretical isotopic pattern (bottom) for $[C_{65}H_{102}N_3O_5]^+$ (**dEt(10)** + H^+) in the ESI-MS measurement.

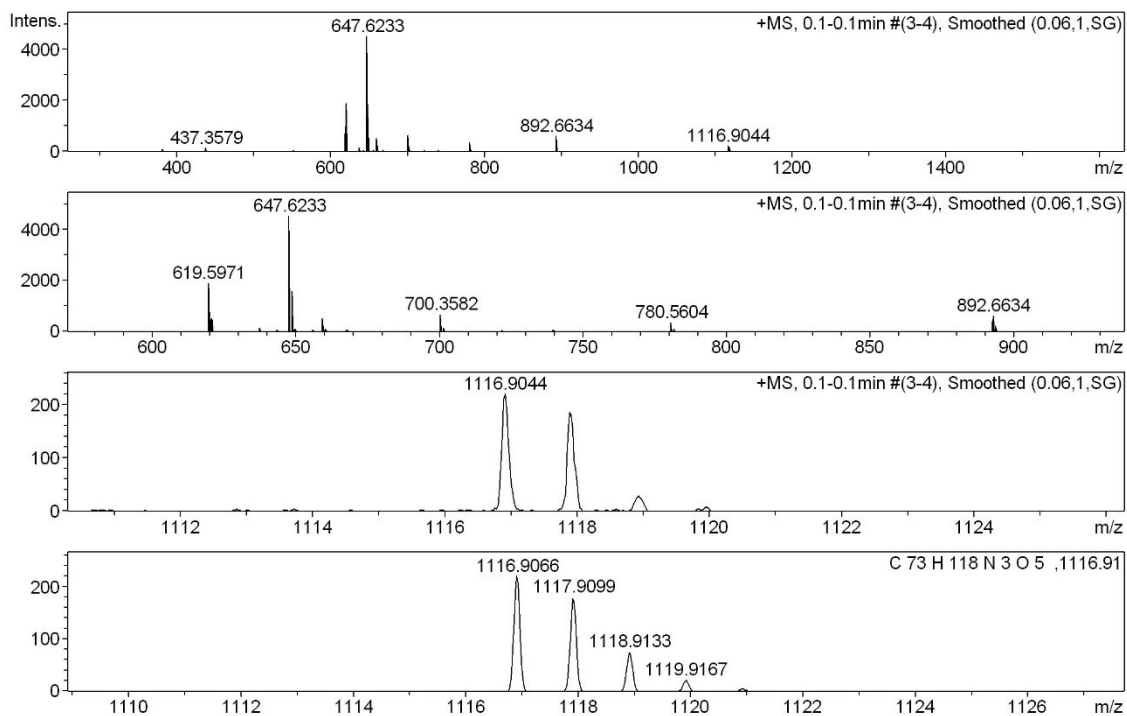


Figure S20. Experimental isotopic patterns of **dEt(12)** (top three patterns) and theoretical isotopic pattern (bottom) for $[C_{73}H_{118}N_3O_5]^+$ (**[dEt(12) + H]⁺**) in the ESI-MS measurement.

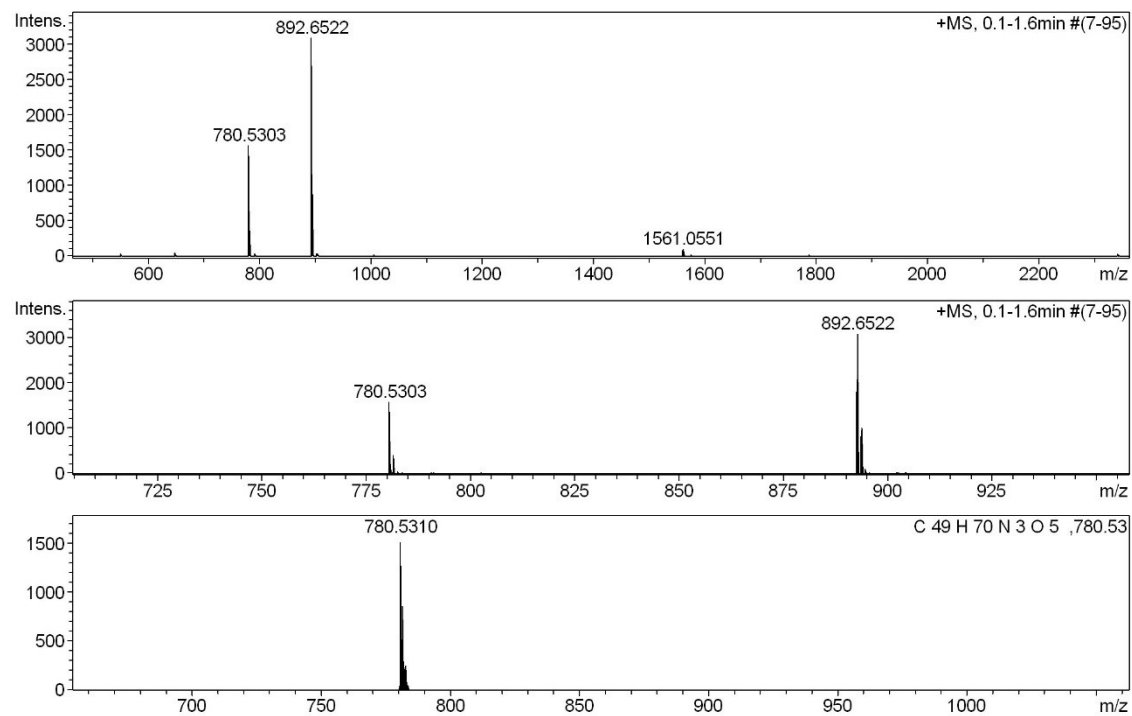


Figure S21. Experimental isotopic patterns of **HBu(6)** (top two patterns) and theoretical isotopic pattern (bottom) for $[C_{49}H_{70}N_3O_5]^+$ ($[HBu(6) + H]^+$) in the ESI-MS measurement.

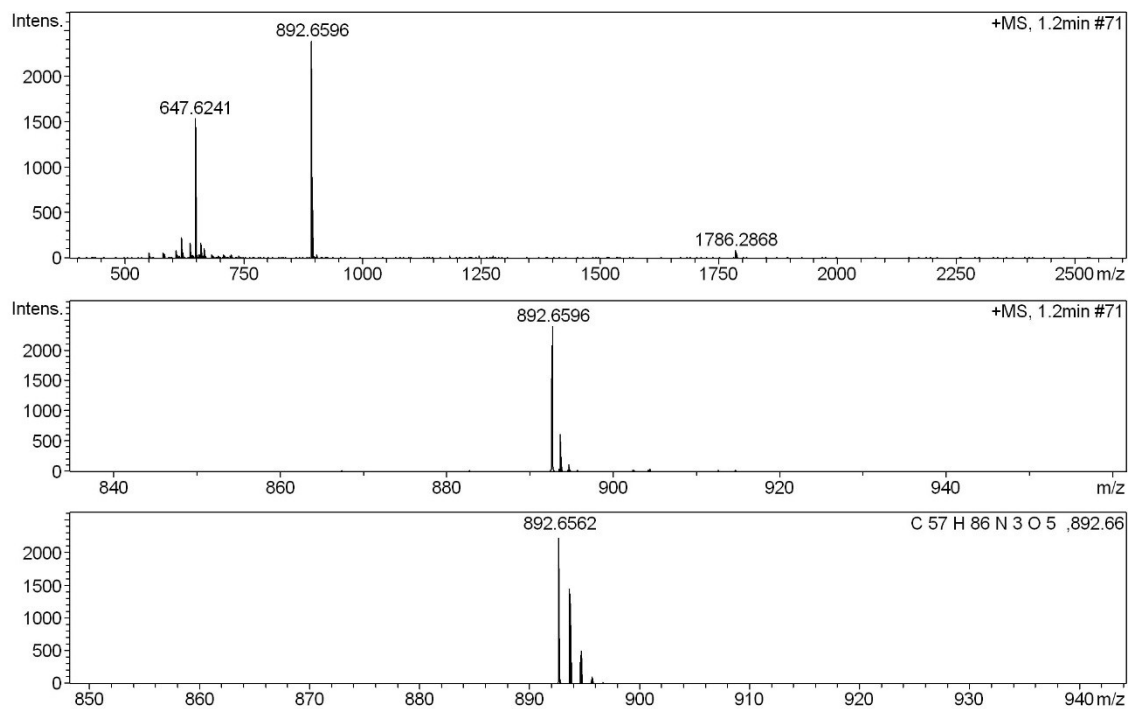


Figure S22. Experimental isotopic patterns of **HBu(8)** (top two patterns) and theoretical isotopic pattern (bottom) for $[C_{57}H_{86}N_3O_5]^+$ ($[HBu(8) + H]^+$) in the ESI-MS measurement.

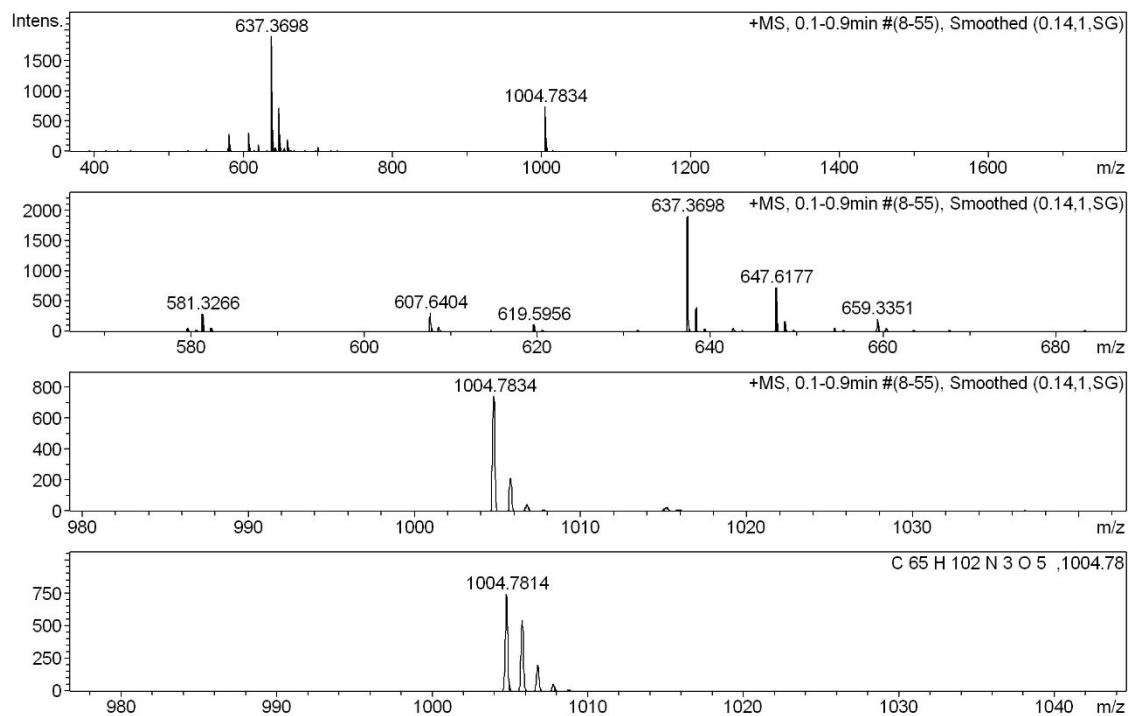


Figure S23. Experimental isotopic patterns of **HBu(10)** (top three patterns) and theoretical isotopic pattern (bottom) for $[\text{C}_{65}\text{H}_{102}\text{N}_3\text{O}_5]^+$ (**HBu(10)** + H^+) in the ESI-MS measurement.

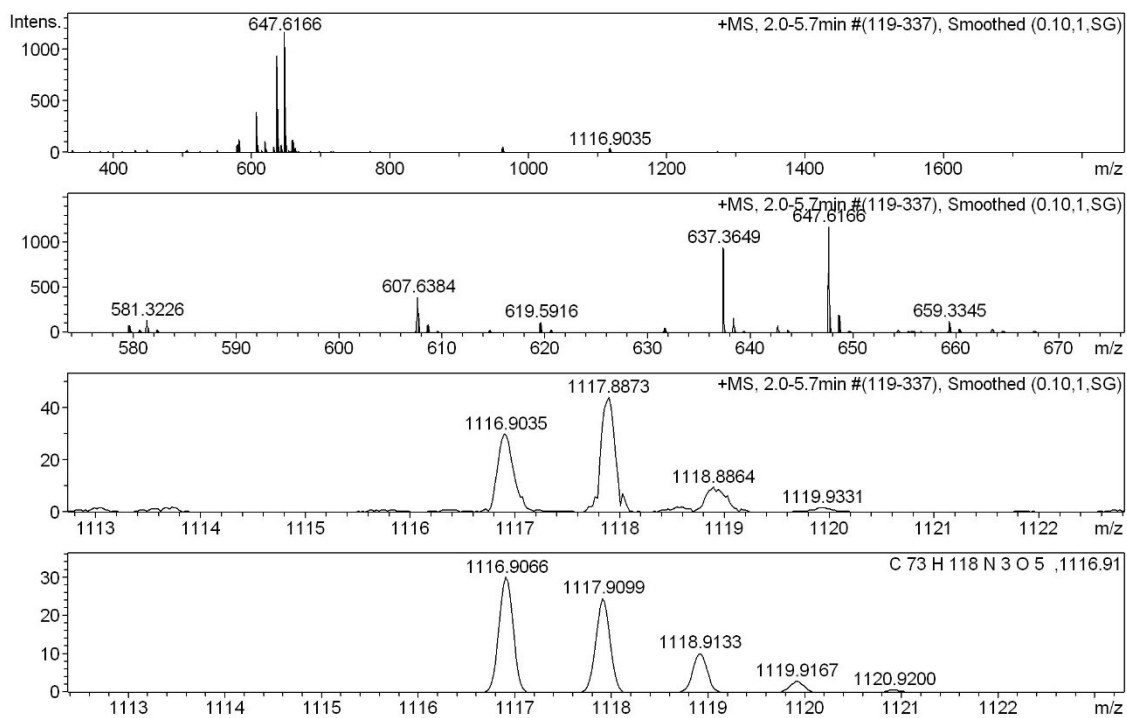


Figure S24. Experimental isotopic patterns of **HBu(12)** (top three patterns) and theoretical isotopic pattern (bottom) for $[C_{73}H_{118}N_3O_5]^+$ (**HBu(12)** + H)⁺ in the ESI-MS measurement.

^1H NMR spectra of **HBu(8)** in the presence of triethylamine.

^1H NMR spectra of **HBu(8)** were measured at several concentrations (19, 58, 116 mM) in the presence of three equivalent of triethyl amine. When the aggregation of **HBu(8)** occurs via impure protons, the presence of triethylamine is expected to change the chemical shifts and shape of the signals at the aromatic regions. However, the spectra at each concentration was almost the same with that measured without triethyl amine, ruling out the possibility that aggregate proceeds via impure protons

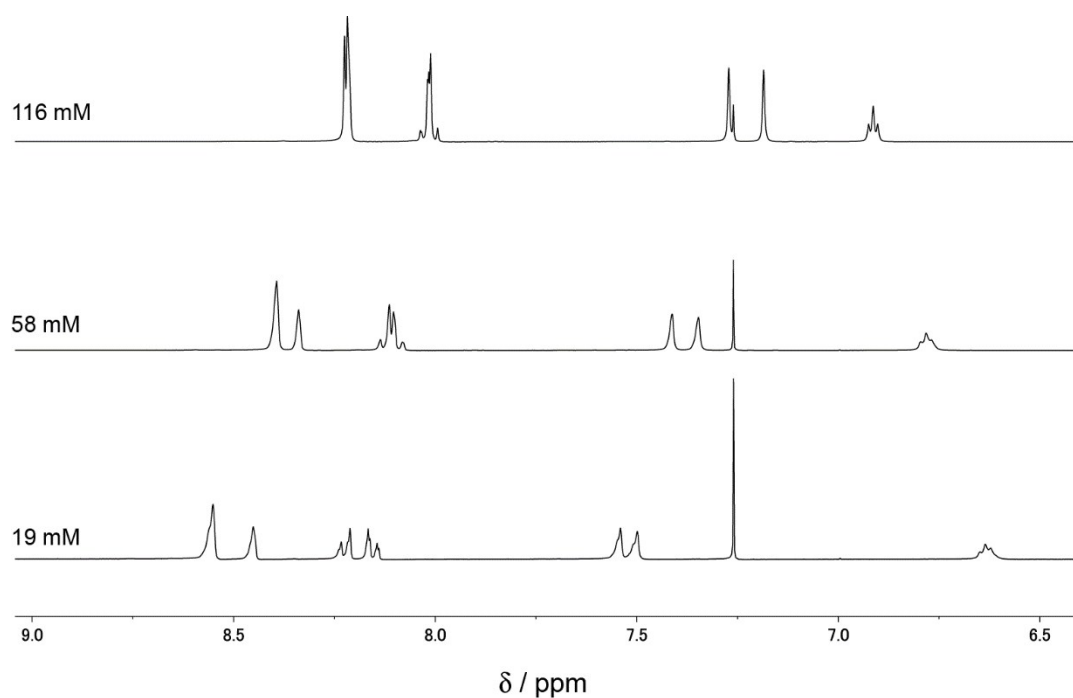


Figure S25. Aromatic region of the ^1H NMR spectra of **HBu(8)** at various concentrations (19, 58, and 116 mM) with 3 equiv. of triethylamine in CDCl_3 .

2D NMR spectroscopy and peak assignments.

Peaks in the aromatic region of the ^1H NMR spectra of **dEt(n)** and **HBu(n)** ($n=6-12$) were assigned using 2D NMR spectroscopy. ^1H NMR spectra of **dEt(n)** were almost identical between 3 and 9 ppm regardless the concentration. For the case of **dEt(n)** series, a full proton assignment using COSY, HMBC and HSQC spectra was only carried out only for **dEt(6)** and **dEt(8)**, but it is assumed to apply to the other **dEt(n)** compounds. Full assignments were carried out for each of **HBu(n)** series and were found to be identical.

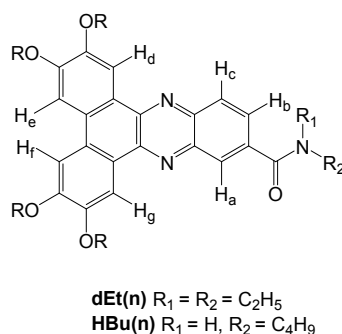


Figure S26. Proton labels for molecules in **dEt(n)** and **HBu(n)** series.

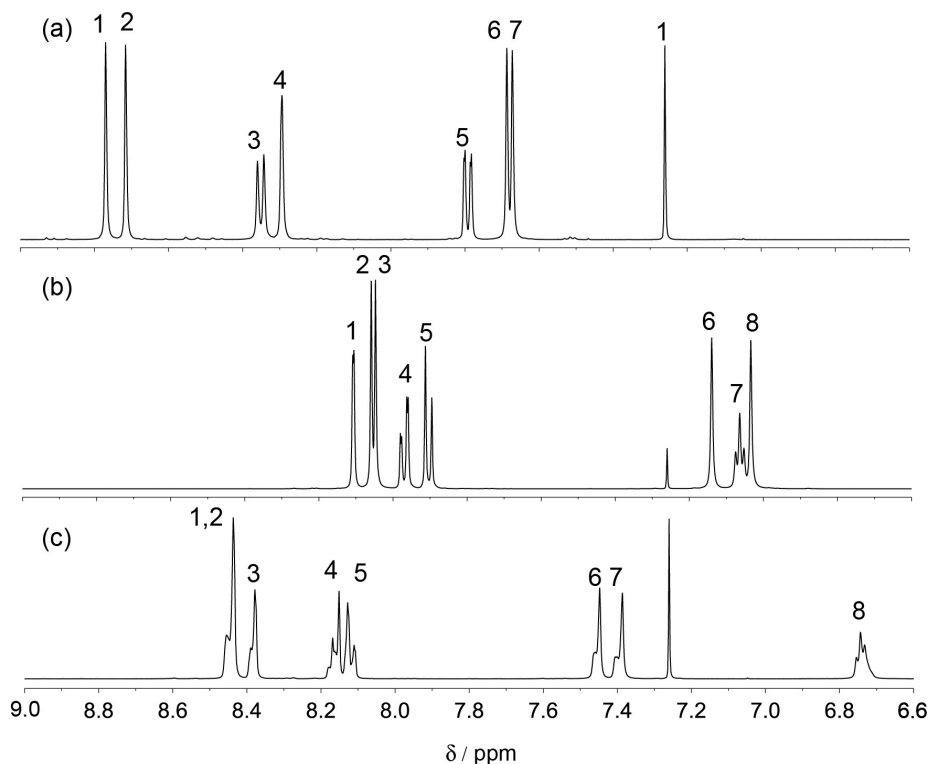


Figure S27. Aromatic region of the ^1H NMR spectra with numbered peaks for a) **dEt(6)** at 60 mM in CDCl_3 , b) **HBu(8)** at 245 mM in CDCl_3 , and **HBu(8)** at 49 mM in CDCl_3 .

Assignment for dEt(6) at 60 mM

The two broad singlets observed around 3.5 ppm correspond to the two CH₂ groups of the diethyl. Peak 4, the singlet, can be straightforwardly assigned as proton H_a, while the doublet (peak 3) and doublet doublet (peaks 5), are H_b or H_c. The four remaining peaks, singlets 1, 2, 6 and 7, correspond to the four protons on the phenanthrene moiety (H_d, H_e, H_f or H_g). The COSY spectrum shows strong coupling between peak 3 and 4 and weak coupling between peak 3 and 5. It follows that doublet doublet 5 is H_b and doublet 3 is H_c, since these H_b is closer to H_a. Protons H_e and H_f are in a very similar environment, as are protons H_d and H_g. Two singlets (peaks 1 and 2) are assigned to H_d and H_g from the analogy of the assignment in **3** based on ROESY spectrum.⁴ Other two singlets (peaks 6 and 7) are assigned to H_e and H_f. HSQC spectrum shows that Peaks 1 and 2 are coupled with two carbons with similar chemical shifts (108.97 and 108.88 ppm), again showing that they are in a very similar environment. In the HMBC spectrum, the carbonyl peak (170.5 ppm) couples with peaks 4 and 5, which confirms their assignment as H_a and H_b, respectively. Discrimination between H_e and H_f and between H_d and H_g was impossible from these experimental results.

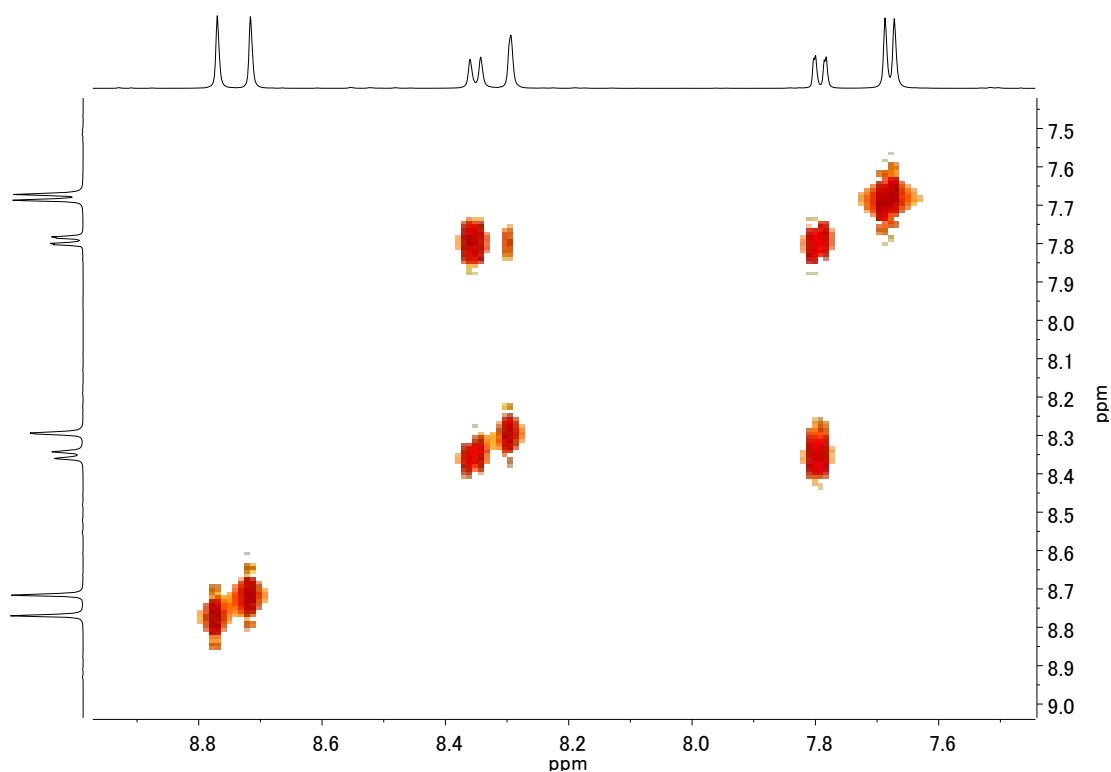


Figure S28. COSY spectrum of dEt(6) at 60 mM in CDCl₃.

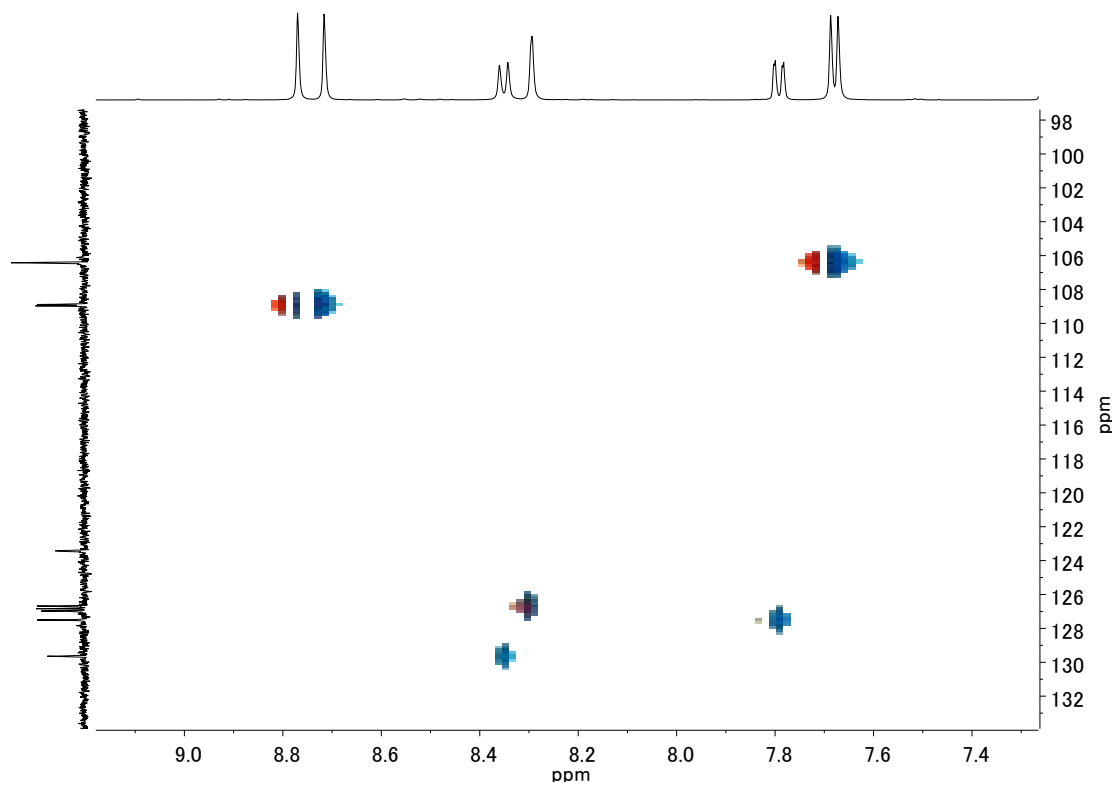


Figure S29. HSQC spectrum of **dEt(6)** at 60 mM in CDCl_3 .

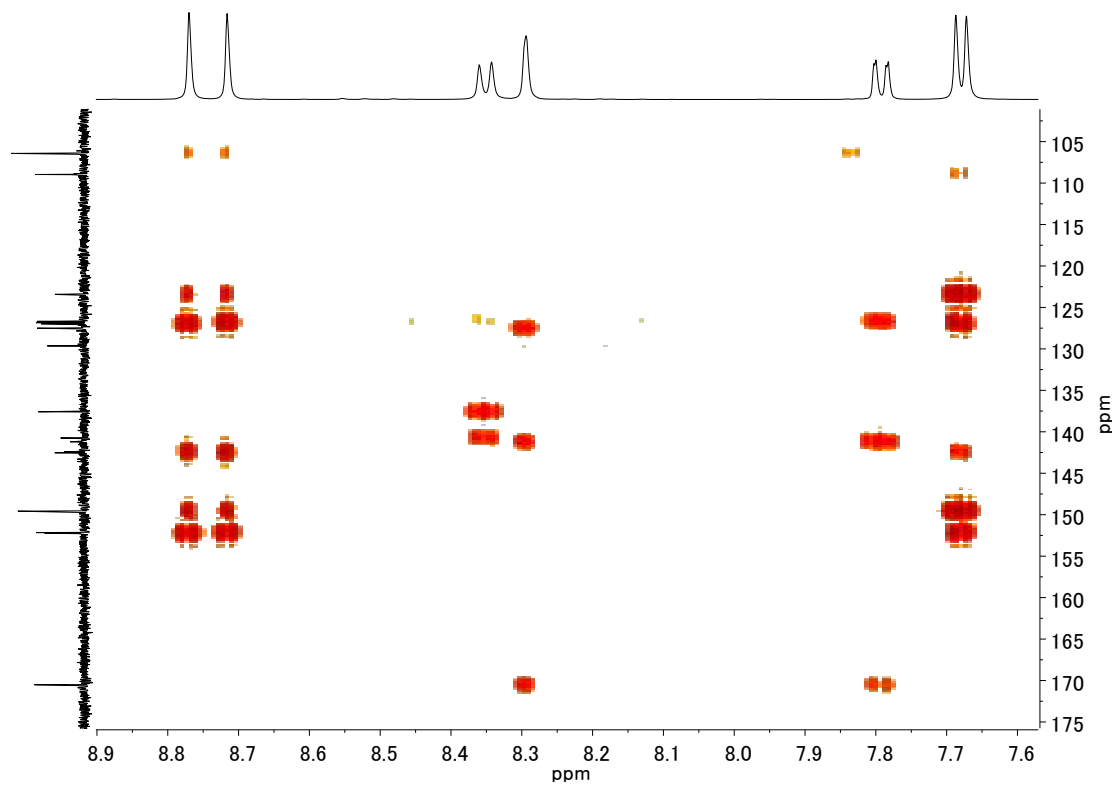


Figure S30. HMBC spectrum of **dEt(6)** at 60 mM in CDCl_3 .

Assignment for HBU(8) at 245 mM

The triplet peak 7 can be assigned as the proton on the NH group. Peak 4, the triplet, should be proton H_b, while the doublets 1 and 2 correspond to protons H_a or H_c. Peak 1, the singlet, can be straightforwardly assigned as proton H_a, while the doublet doublet (peak 4) and doublet (peaks 5), are H_b or H_c. The four remaining peaks, singlets 2, 3, 6 and 8, correspond to the four protons on the phenanthrene moiety (H_d, H_e, H_f or H_g). The COSY spectrum shows strong coupling between peak 4 and 5 and weak coupling between peak 1 and 4. It follows that doublet doublet 4 is H_b and doublet 5 is H_c, since these H_b is closer to H_a. Two singlets (peaks 2 and 3) are assigned to H_d and H_g as the cases of HBU(6). Other two singlets (peaks 6 and 7) are assigned to H_e and H_f. In the HSQC spectrum, peak 6 and 8 are coupled with the carbon peaks at 105.7 and 105.2 ppm, respectively. In contrast, peak 2 and 3 are coupled with the carbon peak at 108.0. The results indicates that environmental difference between H_e and H_f are slightly larger than that of H_d and H_g. In the HMBC spectrum, the carbonyl peak (168.0 ppm) couples with peaks 1 and 5, which confirms their assignment as H_a and H_b, respectively. Discrimination between H_e and H_f and between H_d and H_g was impossible from these experimental results.

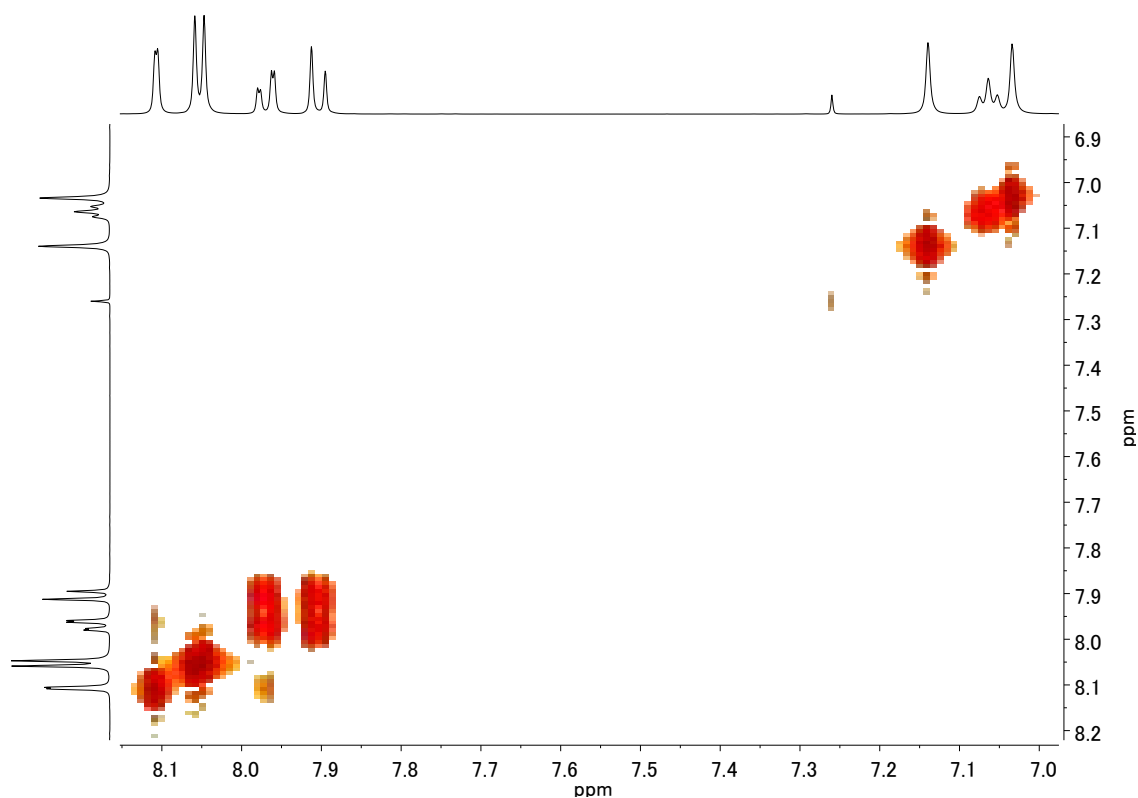


Figure S31. COSY spectrum of HBU(8) at 245 mM in CDCl₃.

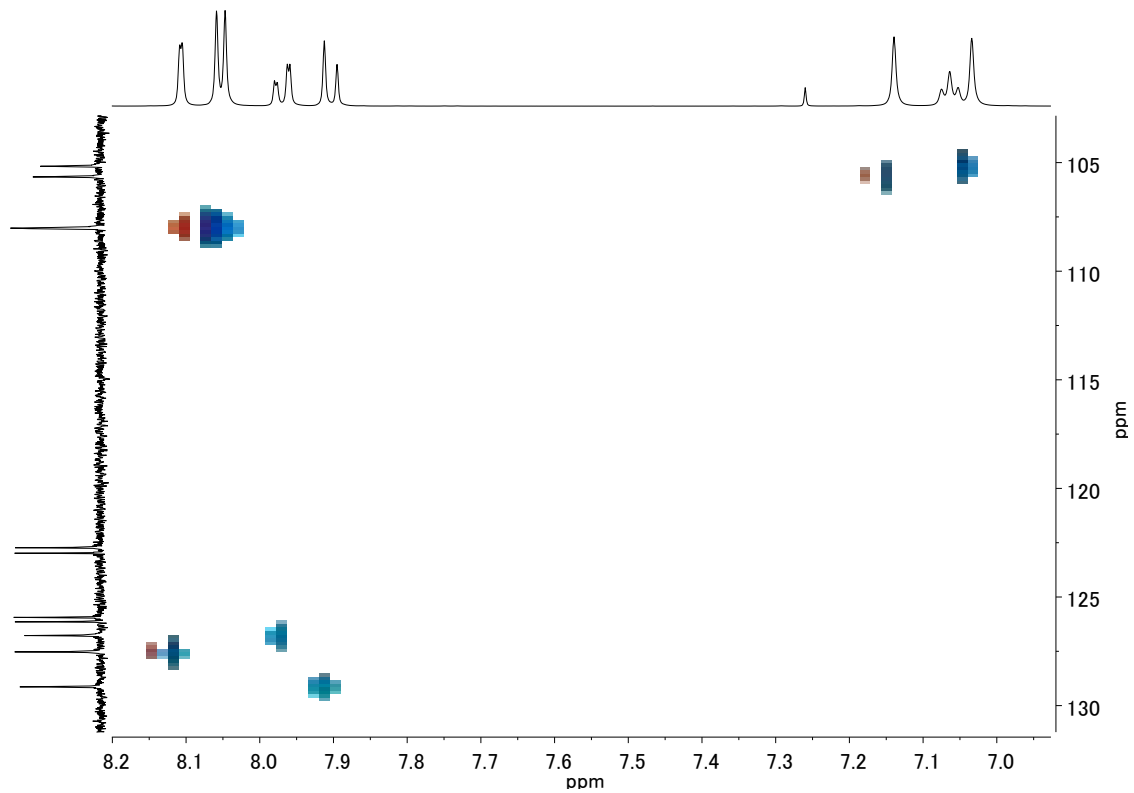


Figure S32. HSQC spectrum of **HBU(8)** at 245 mM in CDCl_3 .

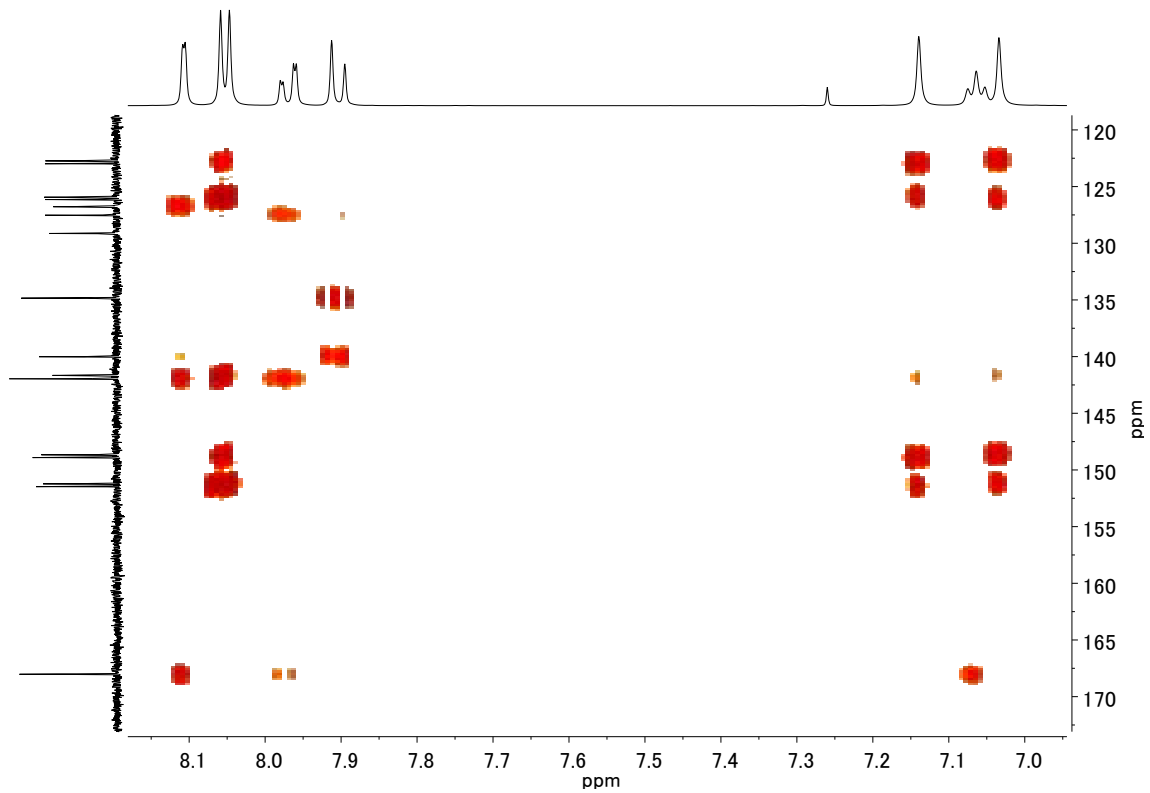


Figure 33. HMBC spectrum of **HBU(8)** at 245 mM in CDCl_3 .

Assignment for H_{Bu}(8) at 49 mM

The assignment could be performed similarly with case at 245 mM. Major difference of the spectra at 245 and 49 mM is the position of H_b, and H_c. From the ¹H NMR and COSY spectra, the peaks 4 and 5 are assigned to H_c and H_b, respectively. The coupling between carbonyl peak (167.6 ppm) with peaks 3 and 5 in the HMBC spectrum confirms the assignment of H_a and H_b.

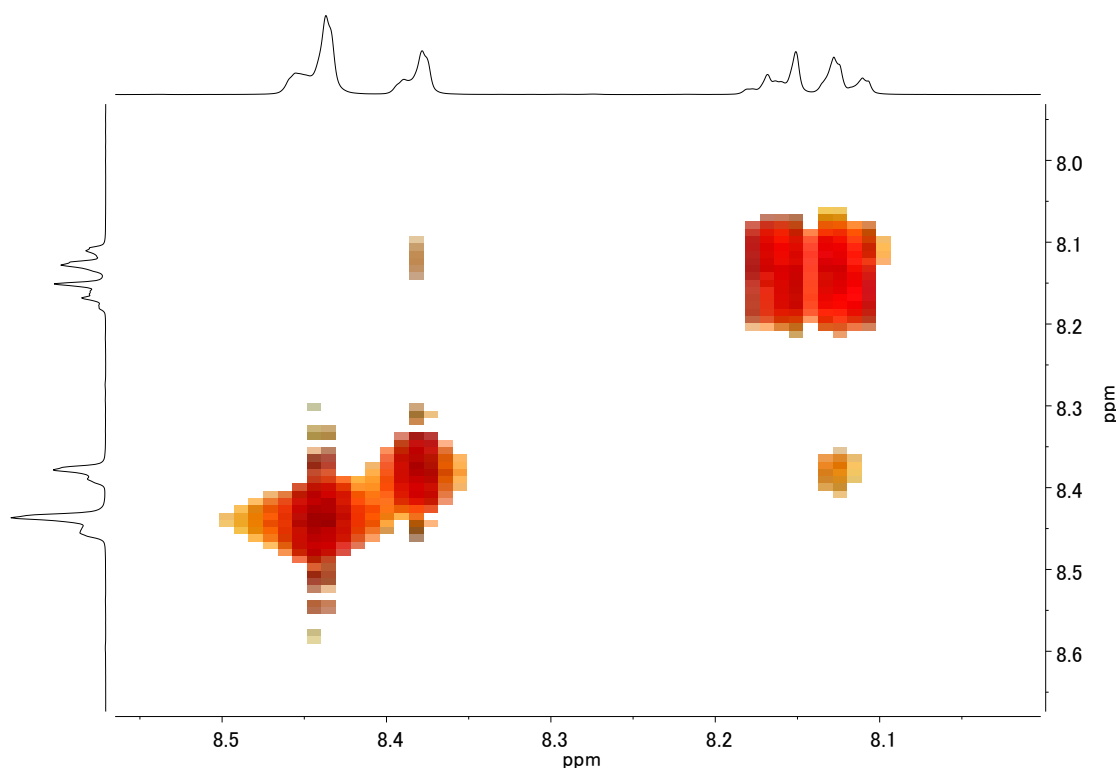


Figure S34. COSY spectrum of H_{Bu}(8) at 49 mM in CDCl₃.

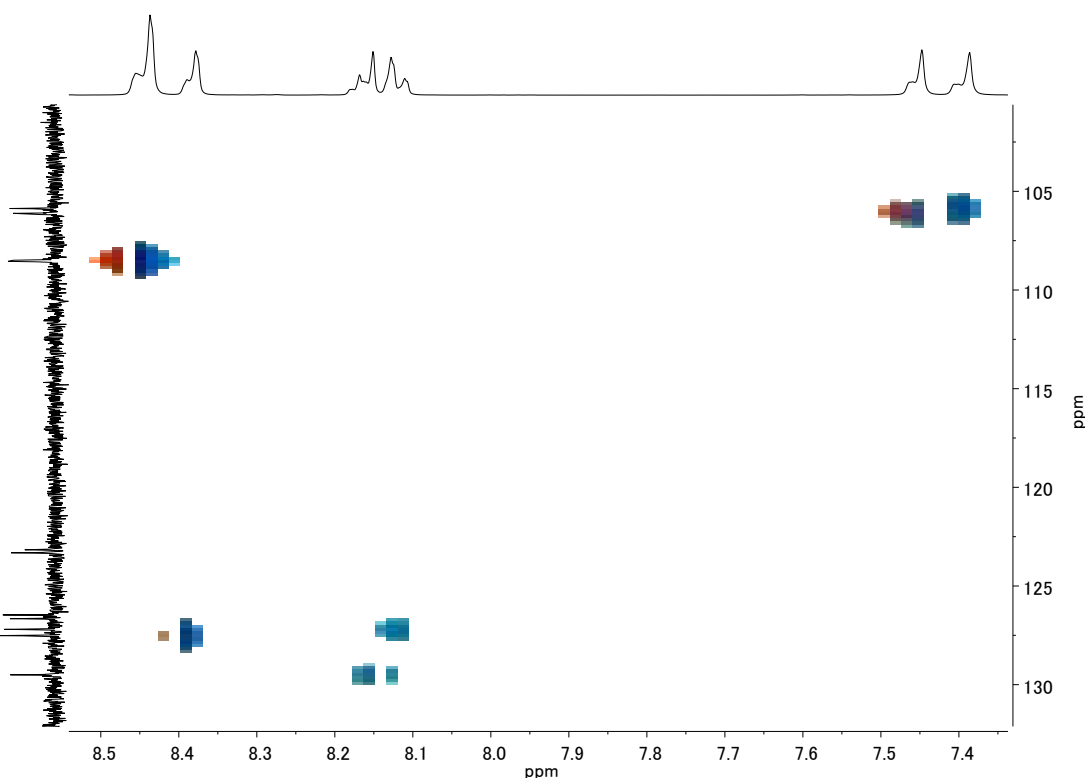


Figure S35. HSQC spectrum of **HBU(8)** at 49 mM in CDCl_3 .

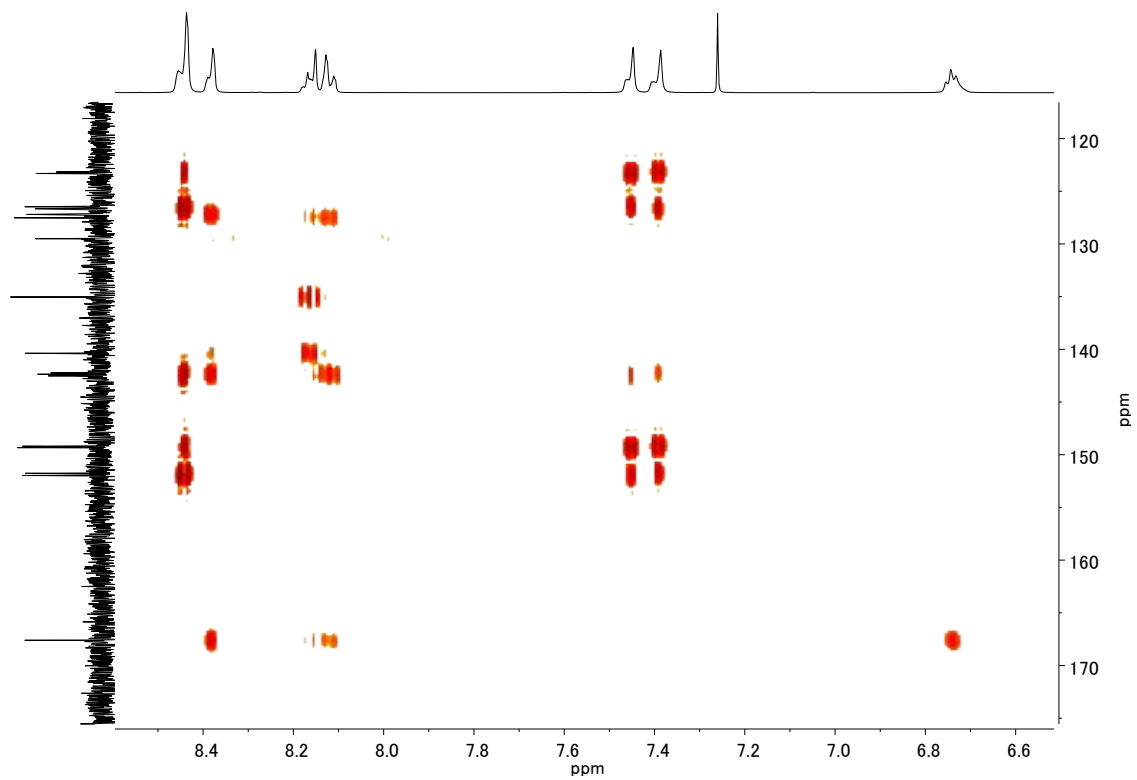


Figure S36. HMBC spectrum of **HBU(8)** at 49 mM in CDCl_3 .

^1H NMR dilution experiments and analysis

Dilution experiments were performed on all molecules in series **dEt(n)** ($n = 6-12$) and **HBu(n)** ($n = 6-12$). A stock solution of the desired compound was prepared in deuterated chloroform (0.045 – 0.056 M for **dEt(n)** ($n = 6-12$), 0.106 – 0.245 M for **HBu(n)** ($n = 6-12$)). Samples at various concentrations were prepared by mixing the stock solution with additional deuterated chloroform placed in a vial. ^1H NMR spectra of **dEt(n)** ($n = 6-12$) show no significant variation with concentration, while those of **HBu(n)** ($n = 6-12$) show explicit upfield shifts with the increase of the concentration.

In order to fit the data to the isodesmic model, the chemical shift of each proton on the monomer had to be estimated. This was done by linear regression on the first two or three data points for each curve. Results were always very close to the values obtained at the lowest measured concentration. Once chemical shifts of the monomer were obtained for **HBu(n)** ($n = 6-12$), the difference in chemical shift ($\delta_{\text{M}} - \delta$) was plotted against concentration. The plots were fitted to the equation (1) using Origin 2019b. Equilibrium constant was set to equal in every proton.

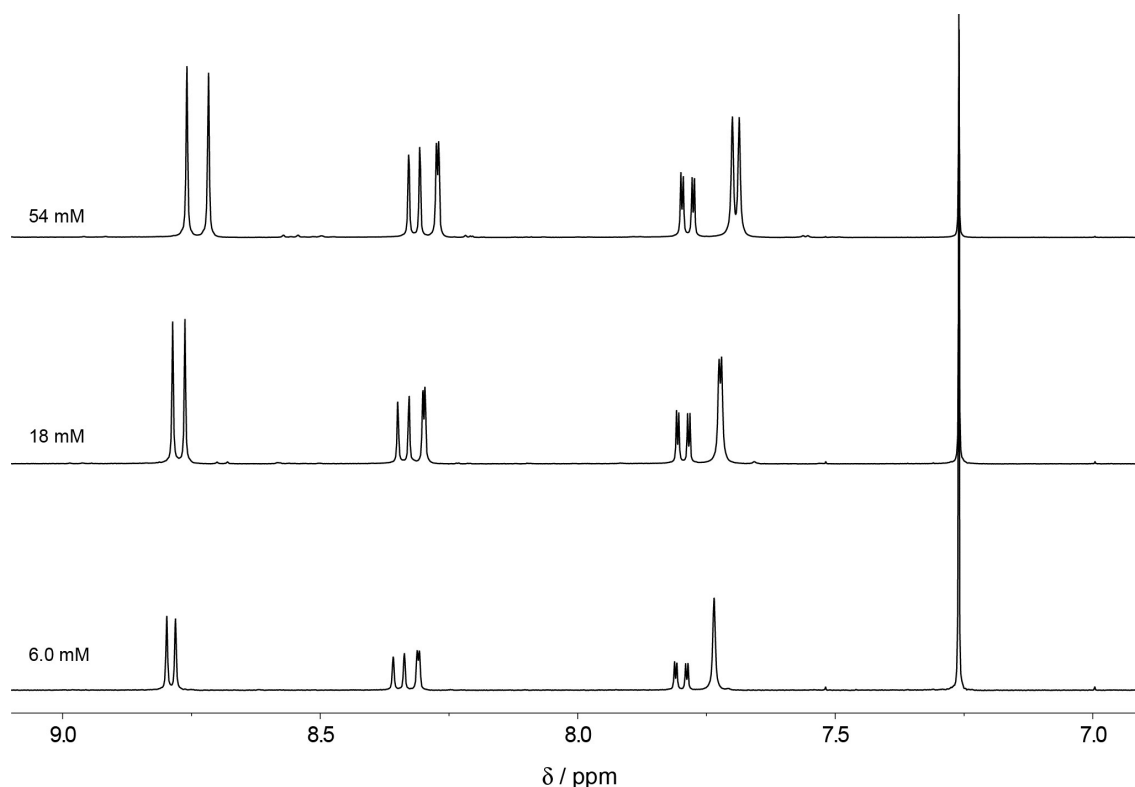


Figure S37. Aromatic region of the ^1H spectra of **dEt(8)** measured at 56, 19, and 6.2 mM in CDCl_3 .

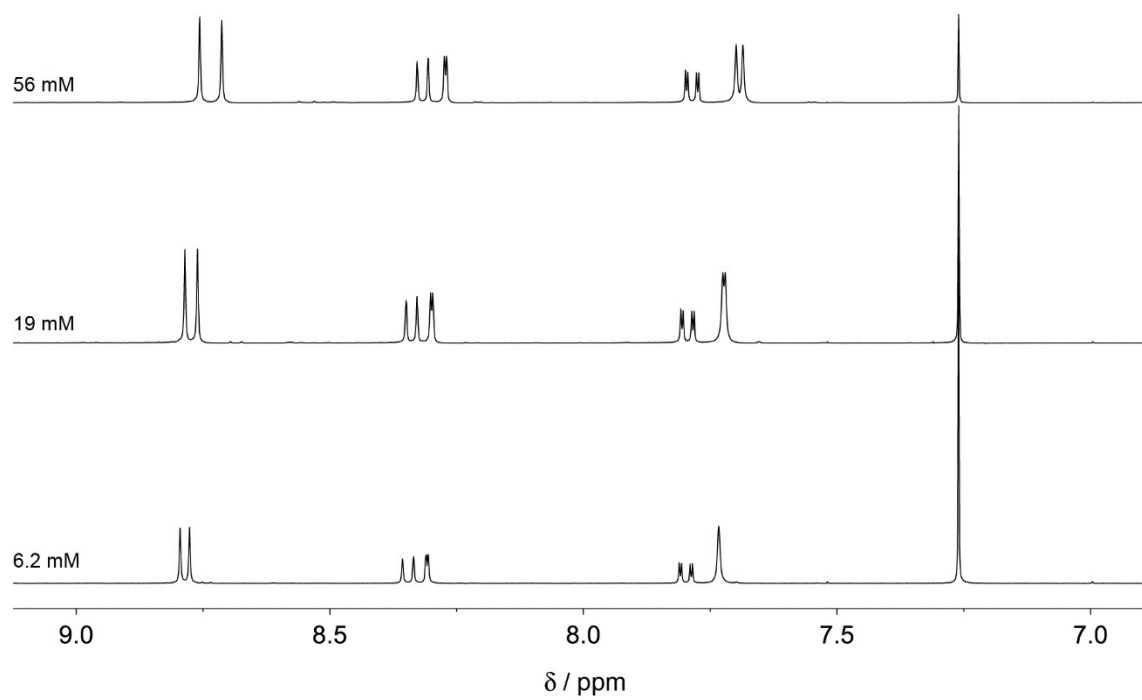


Figure S38. Aromatic region of the ¹H spectra of **dEt(8)** measured at 56, 19, and 6.2 mM in CDCl₃.

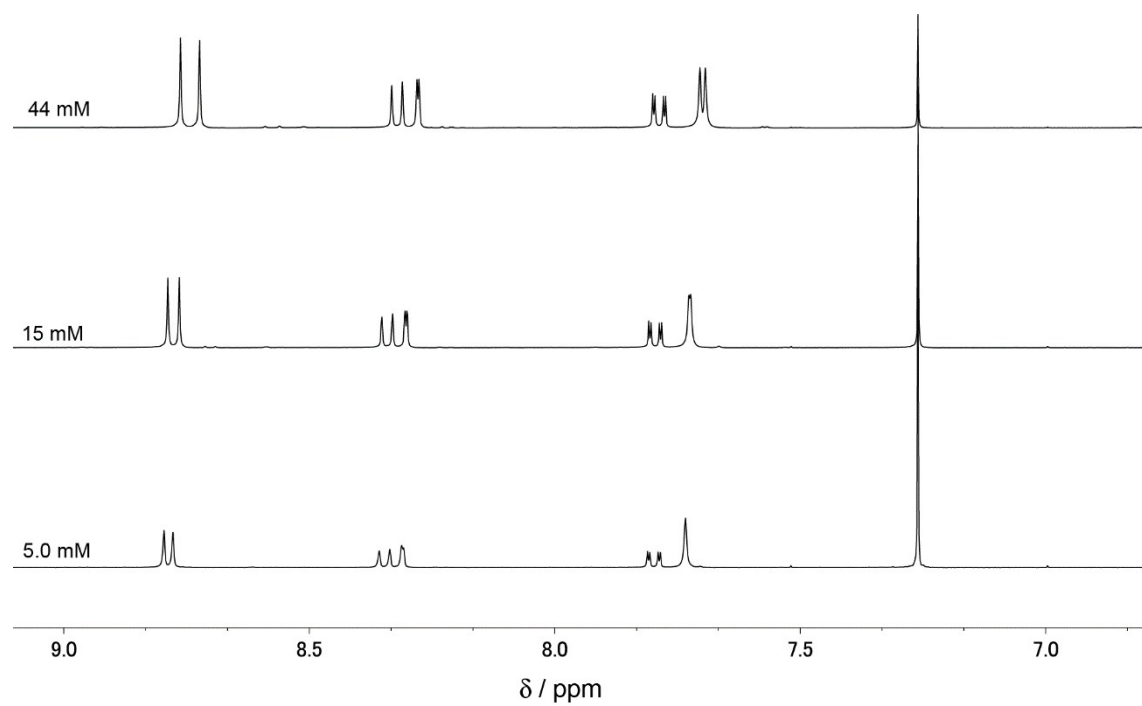


Figure S39. Aromatic region of the ¹H spectra of **dEt(10)** measured at 44, 15, and 5.0 mM in CDCl₃.

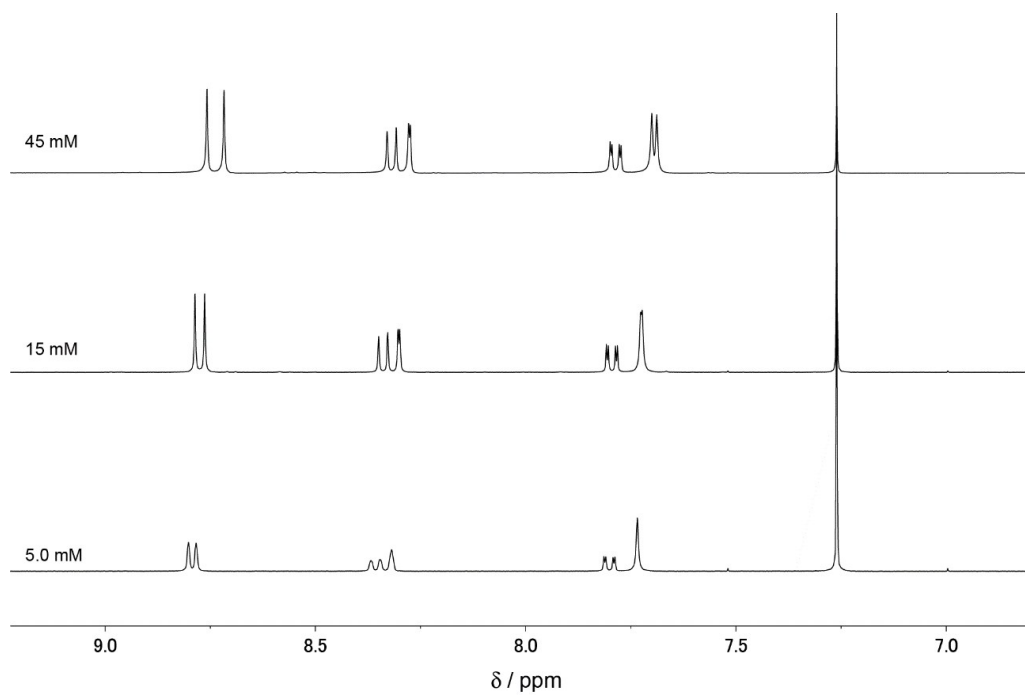


Figure S40. Aromatic region of the ^1H spectra of **dEt(12)** measured at 45, 15, and 5.0 mM in CDCl_3

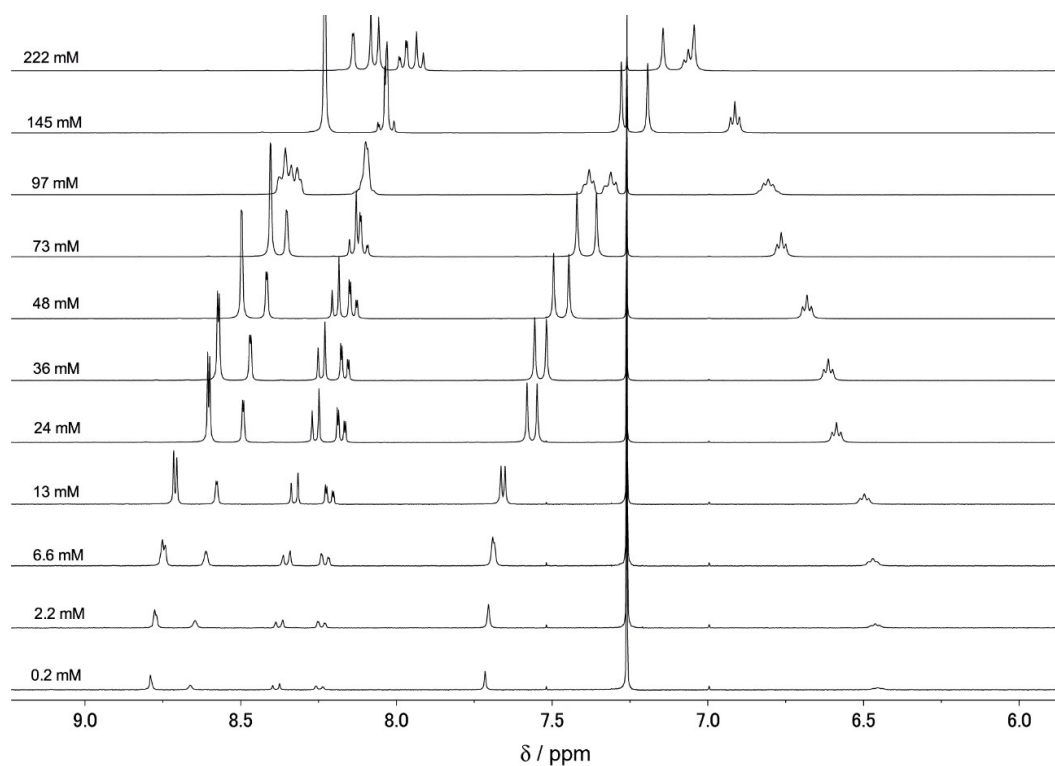


Figure S41. Aromatic region of the ^1H spectra of **HBU(6)** measured at various concentrations from 0.2 to 222 mM in CDCl_3 .

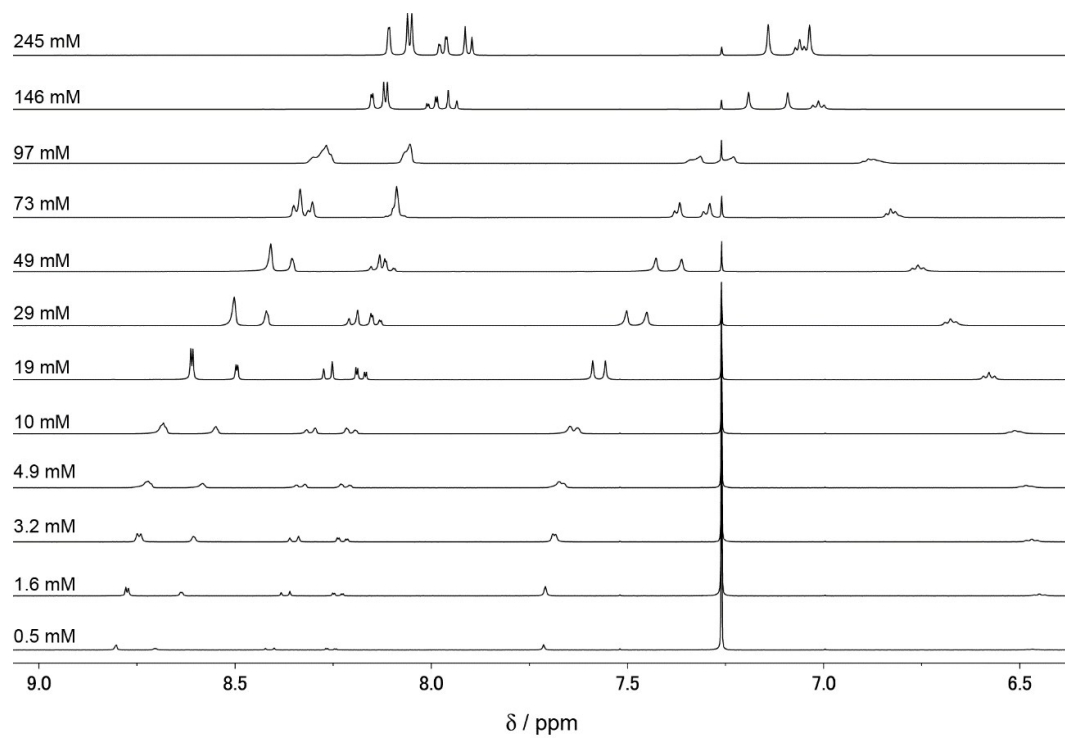


Figure S42. Aromatic region of the ^1H spectra of **HBU(8)** measured at various concentrations from 0.5 to 245 mM in CDCl_3 .

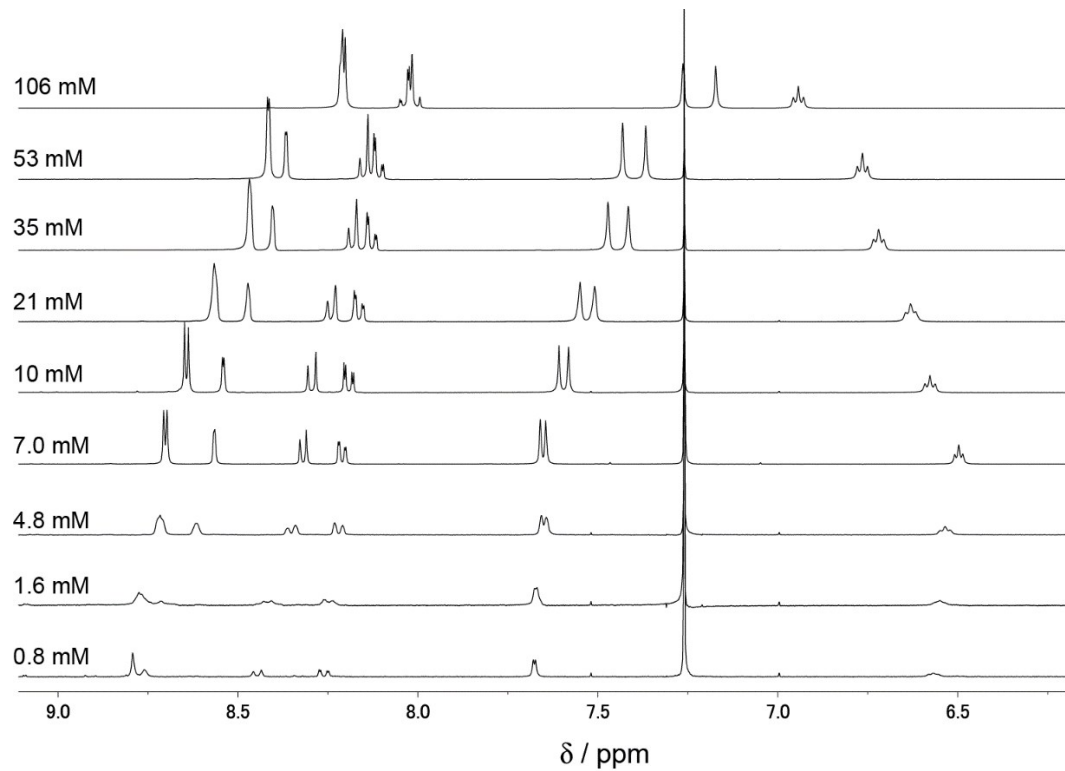


Figure S43. Aromatic region of the ^1H spectra of **HBU(10)** measured at various concentrations from 0.8 to 106 mM in CDCl_3 .

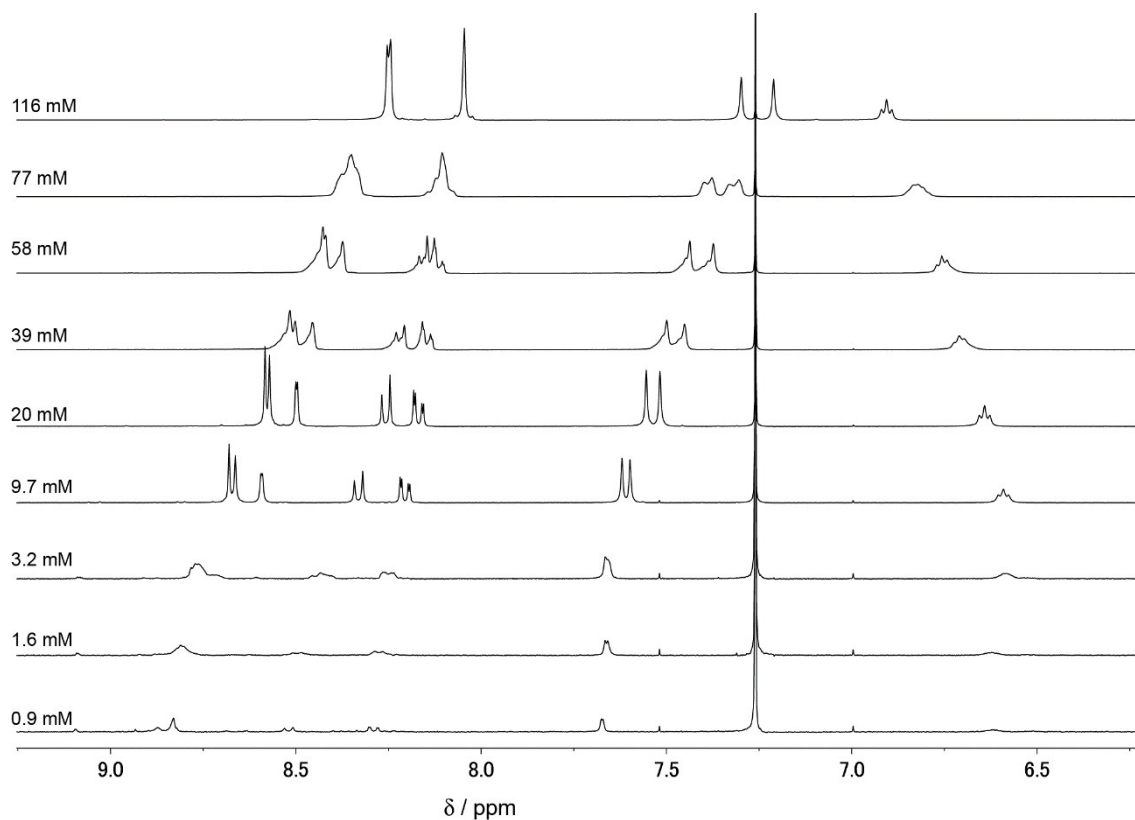


Figure S44. Aromatic region of the ^1H spectra of **HBu(12)** measured at various concentrations from 0.9 to 116 mM in CDCl_3 .

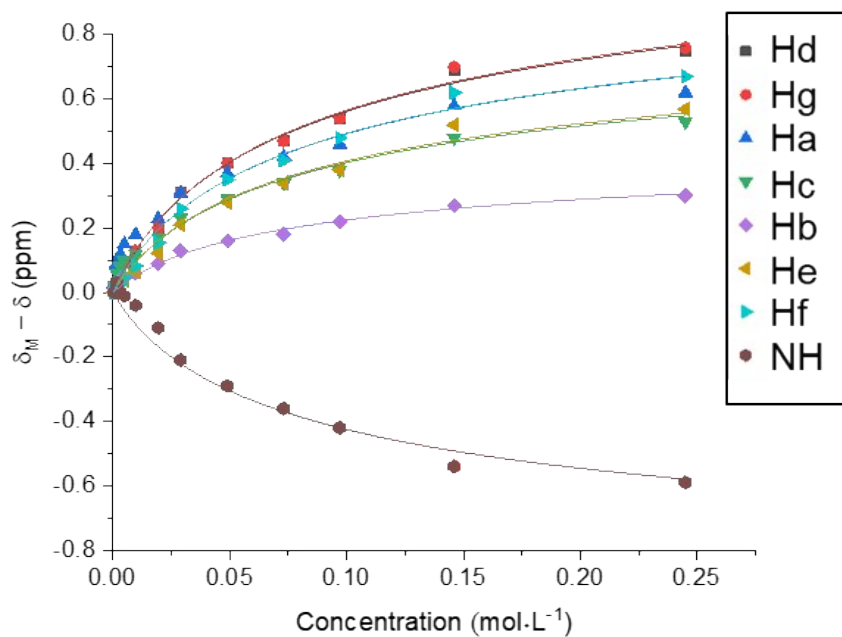


Figure S45. Changes in chemical shift versus concentration in CDCl_3 for **HBu(8)**. Fitting curves were calculated based on the isodesmic model.

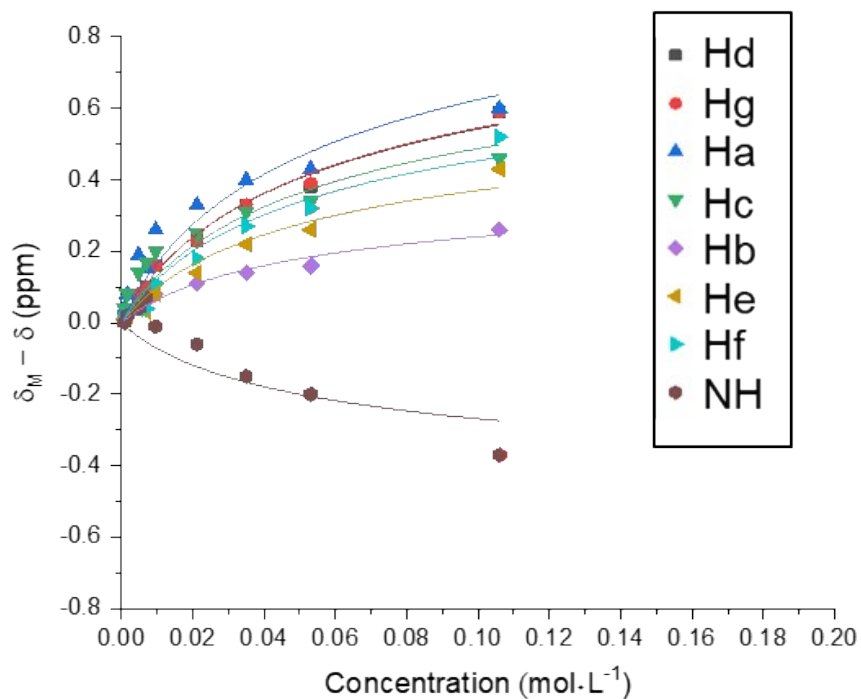


Figure S46. Changes in chemical shift versus concentration in CDCl₃ for **HBu(10)**. Fitting curves were calculated based on the isodesmic model.

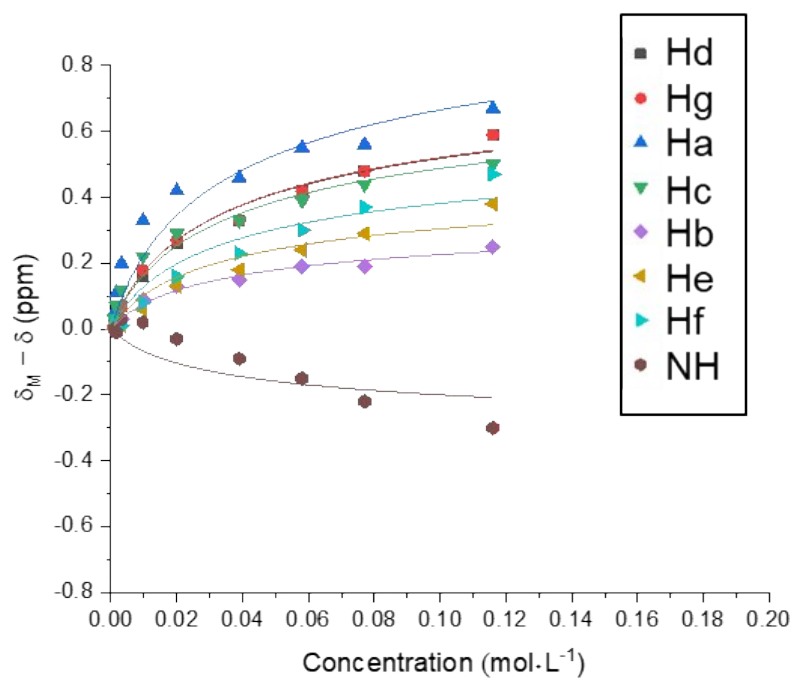


Figure S47. Changes in chemical shift versus concentration in CDCl₃ for **HBu(12)**. Fitting curves were calculated based on the isodesmic model.

Table S1. Maximal chemical shifts of aromatic (H_{a-g}) and NH protons for the solute in an aggregate, equilibrium constant (K_d), and chi-square obtained from the fitting for **HBu(n)** ($n = 6-12$). Letters refer to labels shown in Figure S26.

| | H_a | H_b | H_c | H_d | H_e | H_f | H_g | NH | K_d | Residual sum of χ^2 |
|----------------|-----------------------|-----------------------|-----------------------|-----------------------|-----------------------|-----------------------|-----------------------|-----------------------|----------------------|-----------------------------|
| HBu(6) | 7.11 \pm 0.07 | 7.49 \pm 0.04 | 7.06 \pm 0.06 | 6.77 \pm 0.09 | 6.05 \pm 0.07 | 5.82 \pm 0.08 | 6.77 \pm 0.09 | 8.08 \pm 0.07 | 3.8 \pm 0.3 | 0.022 |
| HBu(8) | 7.54 \pm 0.05 | 7.72 \pm 0.03 | 7.45 \pm 0.04 | 7.45 \pm 0.05 | 6.72 \pm 0.04 | 6.51 \pm 0.05 | 7.44 \pm 0.05 | 7.50 \pm 0.04 | 12.0 \pm 0.9 | 0.079 |
| HBu(10) | 7.45 \pm 0.12 | 7.75 \pm 0.07 | 7.44 \pm 0.10 | 7.63 \pm 0.11 | 6.89 \pm 0.09 | 6.71 \pm 0.10 | 7.62 \pm 0.11 | 7.15 \pm 0.07 | 16.2 \pm 2.7 | 0.114 |
| HBu(12) | 7.76 \pm 0.08 | 7.90 \pm 0.05 | 7.68 \pm 0.06 | 7.93 \pm 0.07 | 7.14 \pm 0.05 | 7.00 \pm 0.06 | 7.93 \pm 0.07 | 6.99 \pm 0.04 | 28.8 \pm 4.7 | 0.110 |

Single crystal X-ray diffraction study

The crystal structure of **dEt(6)** was determined by the single-crystal X-ray diffraction method. A Rigaku XtaLAB Synergy-S (Cu-K α radiation) with a HyPix-6000 area detector was used for the data collection. The structures were solved using the program *SHELXT*.⁵ The refinement and all further calculations were carried out using the program *SHELXL*⁶ via *OLEX2*.⁷ All H atoms were generated geometrically.

Table S2 Crystallographic and experimental data for **dEt(6)**.

| Compound | dEt(6) |
|--|---|
| Formula | C ₄₉ H ₆₉ N ₃ O ₅ |
| Formula weight | 780.07 |
| Crystal system | Triclinic |
| Space group | <i>P</i> -1 |
| <i>a</i> / Å | 11.0975(2) |
| <i>b</i> / Å | 12.3684(3) |
| <i>c</i> / Å | 17.5431(3) |
| α / ° | 108.5460(18) |
| β / ° | 98.9675(18) |
| γ / ° | 95.1364(17) |
| <i>V</i> / Å ³ | 2229.97(8) |
| <i>Z</i> | 2 |
| <i>D</i> _c / Mg m ⁻³ | 1.131 |
| <i>T</i> / K | 173(2) |
| Dimensions / mm | 0.3, 0.1, 0.05 |
| μ (Cu-K α) / mm ⁻¹ | 0.582 |
| F(000) | 848 |
| Reflections collected | 23839 |
| Unique reflections | 8828 |
| Reflections with <i>I</i> > 2 σ (<i>I</i>) | 6734 |
| Parameters | 520 |
| GOF on F ² | 1.066 |
| ^a <i>R</i> ₁ [<i>F</i> ² > 2 σ (<i>F</i> ²)] | 0.0702 |
| ^b <i>wR</i> ₂ (all data) | 0.1974 |

$${}^a R_1 = \frac{\Sigma(|F_o| - |F_c|)}{\Sigma|F_o|}, {}^b wR_2 = \left\{ \frac{\Sigma[w(F_o^2 - F_c^2)^2]}{\Sigma[w(F_o^2)^2]} \right\}^{1/2}$$

DSC data

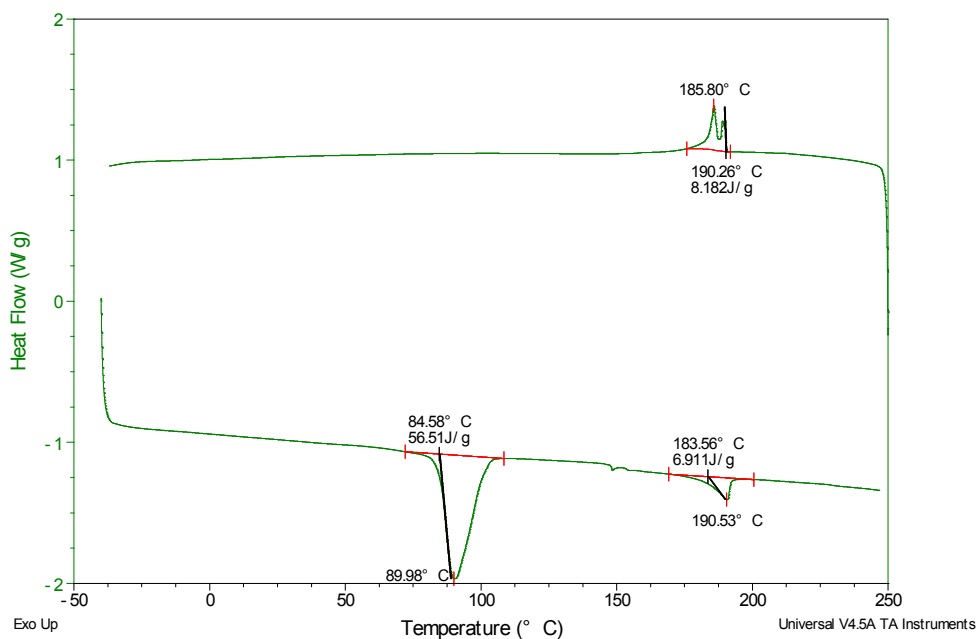


Figure S48. DSC trace (1st scan) for dEt(6) with a heating and cooling rate of 10 °C min⁻¹.

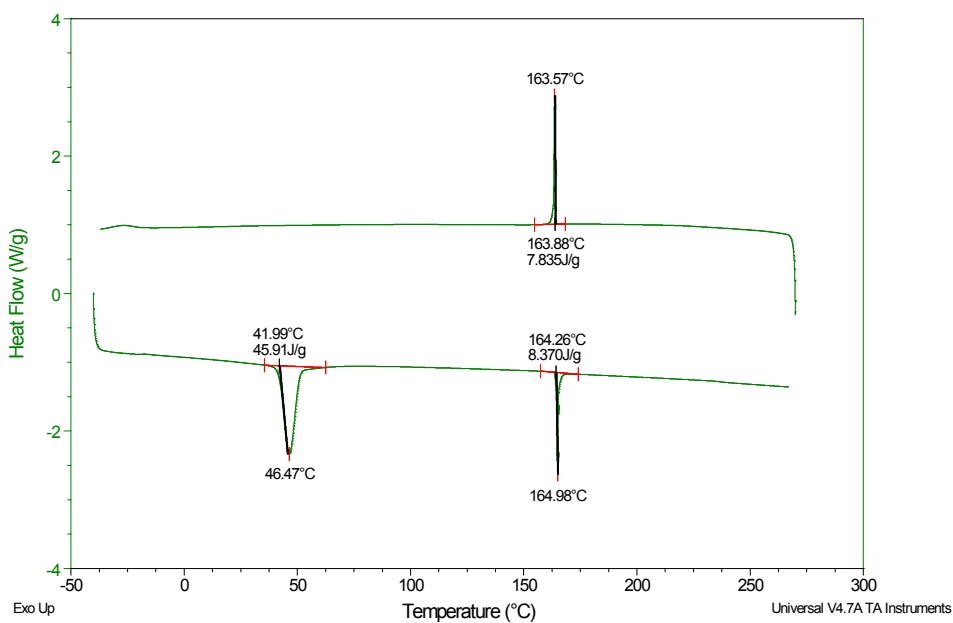


Figure S49. DSC trace (1st scan) for dEt(8) with a heating and cooling rate of 10 °C min⁻¹.

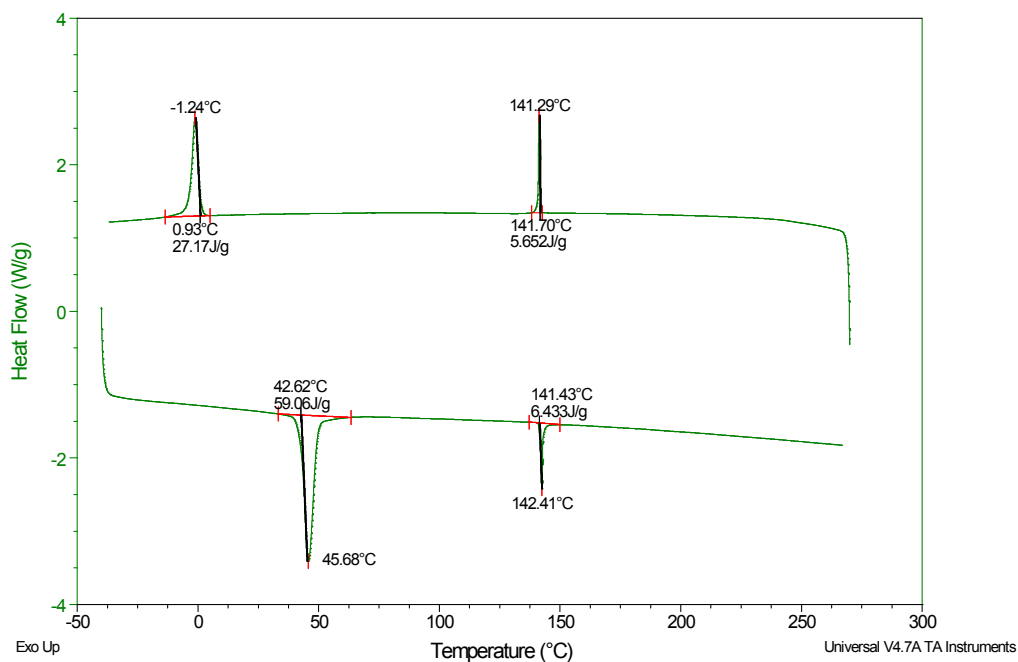


Figure S50. DSC trace (1st scan) for dEt(10) with a heating and cooling rate of 10 °C min⁻¹.

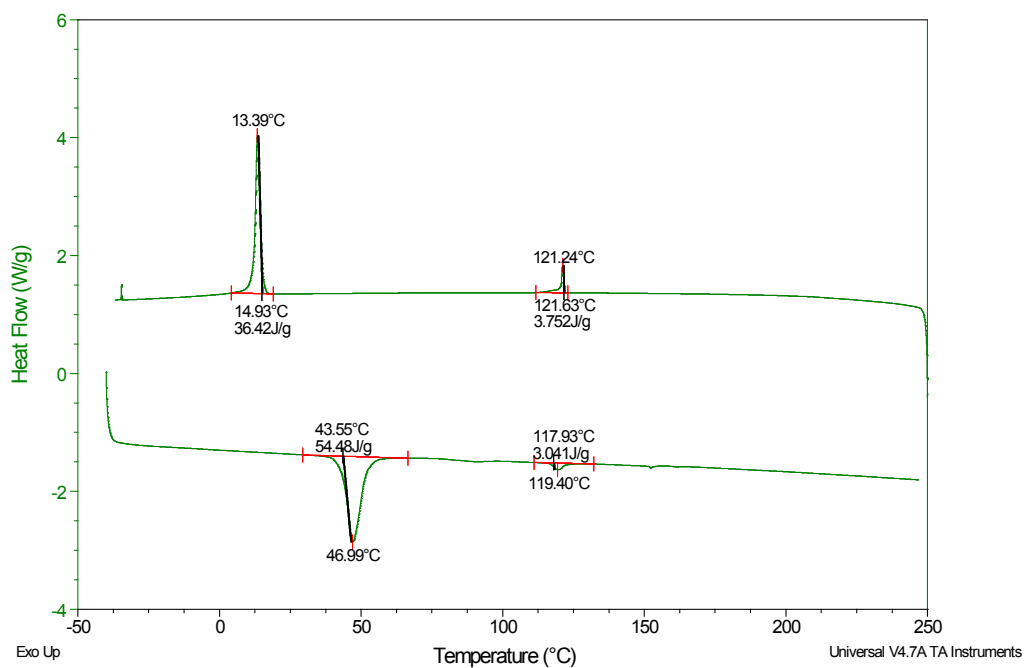


Figure S51. DSC trace (1st scan) for dEt(12) with a heating and cooling rate of 10 °C min⁻¹.

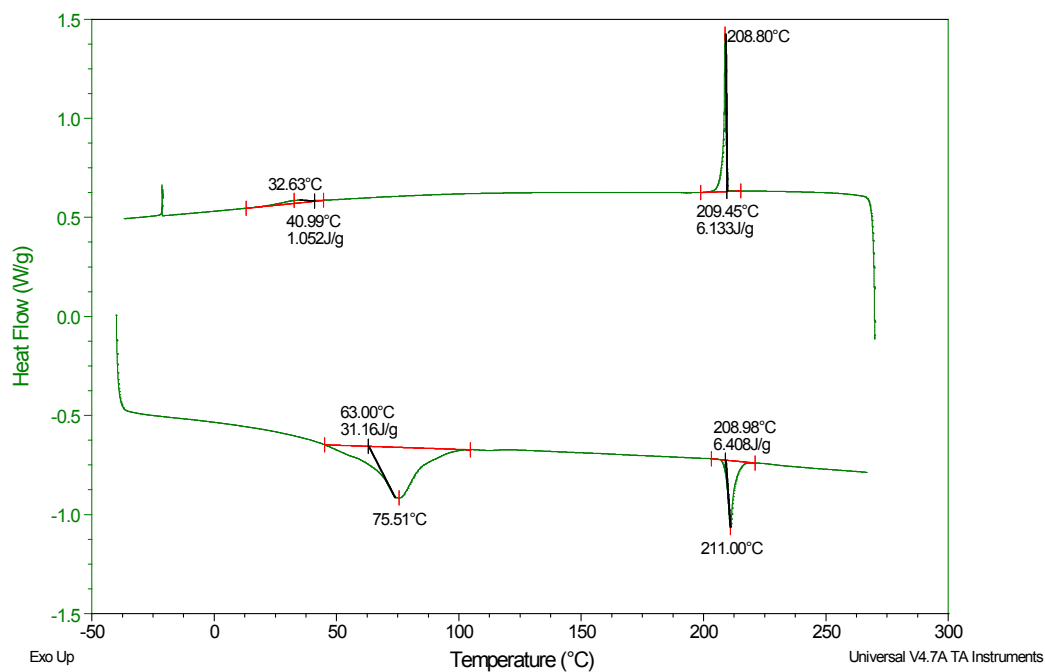


Figure S52. DSC trace (1st scan) for **HBu(6)** with a heating and cooling rate of 10 °C min⁻¹.

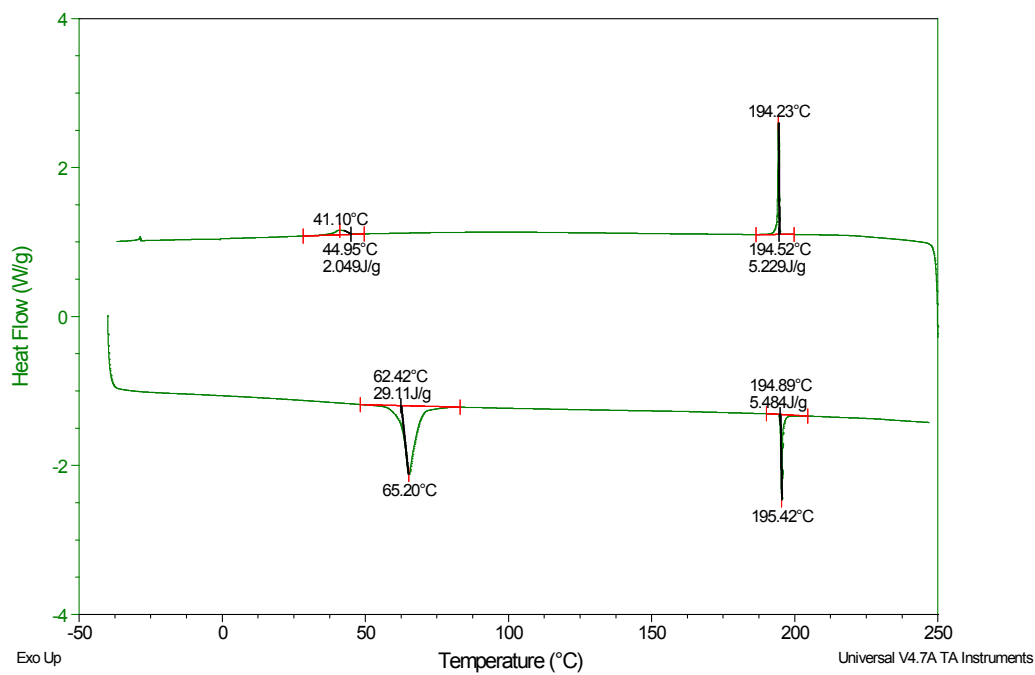


Figure S53. DSC trace (1st scan) for **HBu(8)** with a heating and cooling rate of 10 °C min⁻¹.

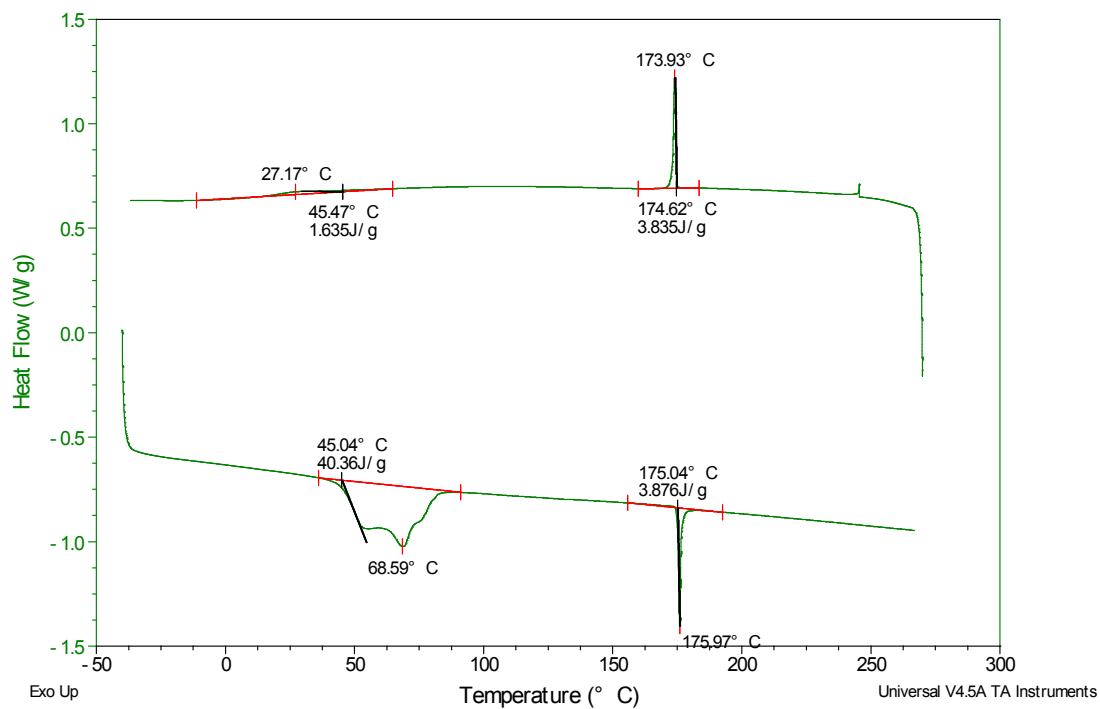


Figure S54. DSC trace (1st scan) for **HBU(10)** with a heating and cooling rate of 10 °C min⁻¹.

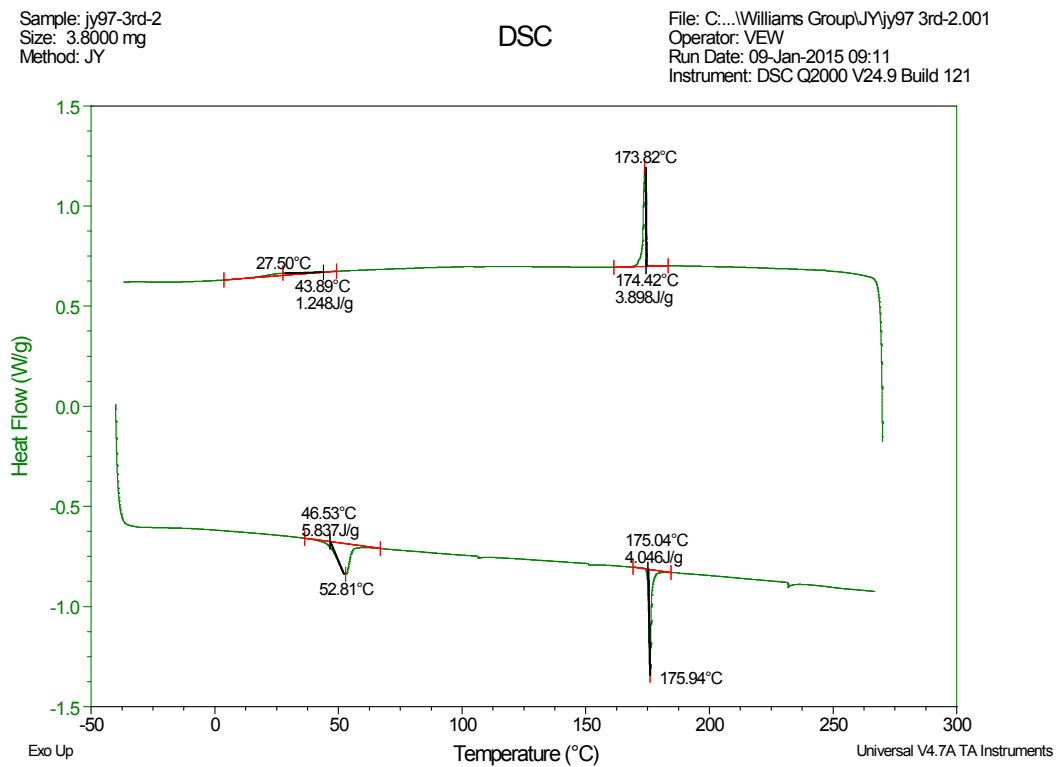


Figure S55. DSC trace (2nd scan) for **HBU(10)** with a heating and cooling rate of 10 °C min⁻¹.

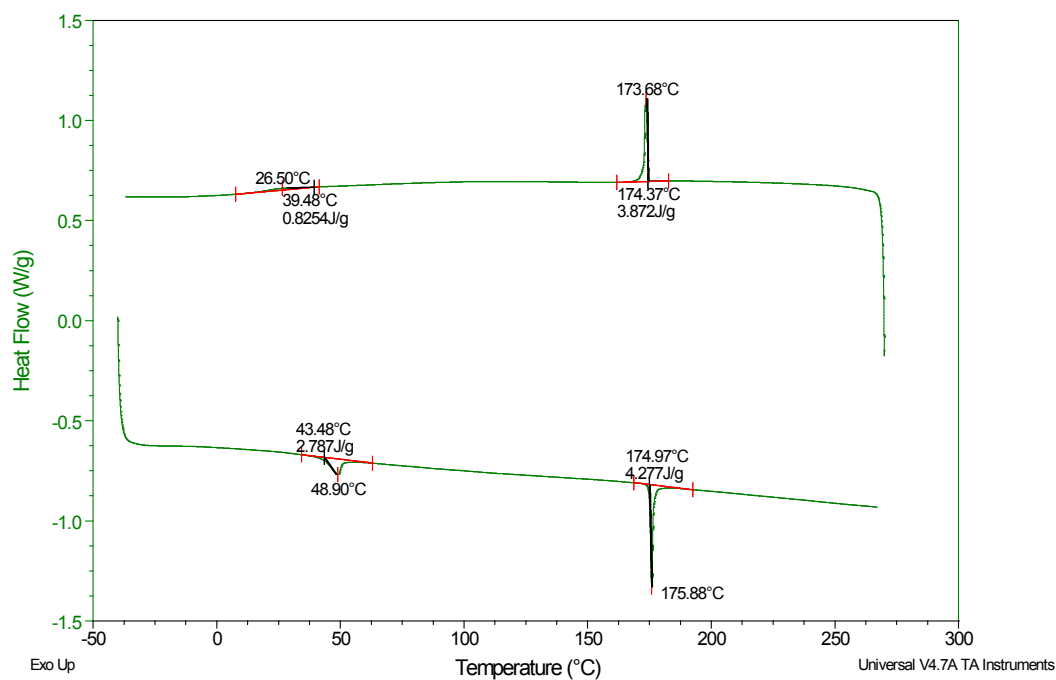


Figure S56. DSC trace (3rd scan) for **HBu(10)** with a heating and cooling rate of 10 °C min⁻¹.

Sample: jy123-1st
 Size: 1.8000 mg
 Method: JY

DSC

File: E:\... DSC raw data SFU\jy123-1st.001
 Operator: VEW
 Run Date: 31- Oct- 2014 10:07
 Instrument: DSC Q2000 V24.9 Build 121

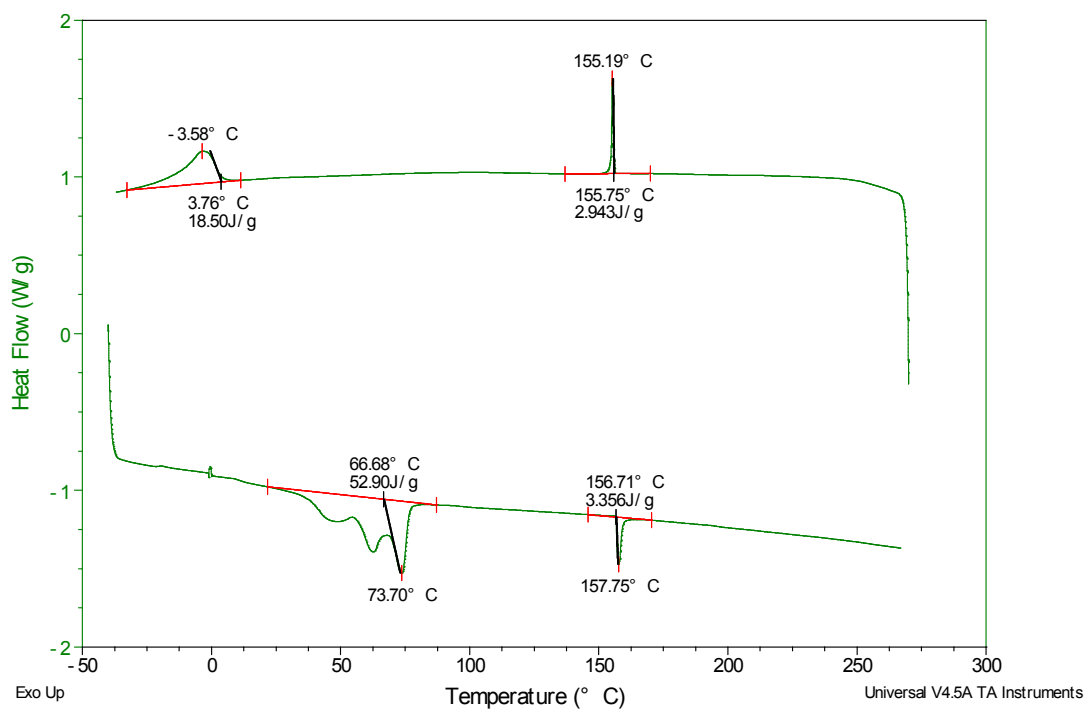


Figure S57. DSC trace (1st scan) for **HBu(12)** with a heating and cooling rate of 10 °C min⁻¹.

Sample: jy123-2nd
Size: 1.8000 mg
Method: JY

DSC

File: C:\...Williams Group\JY\jy123-1st.002
Operator: VEW
Run Date: 31-Oct-2014 11:15
Instrument: DSC Q2000 V24.9 Build 121

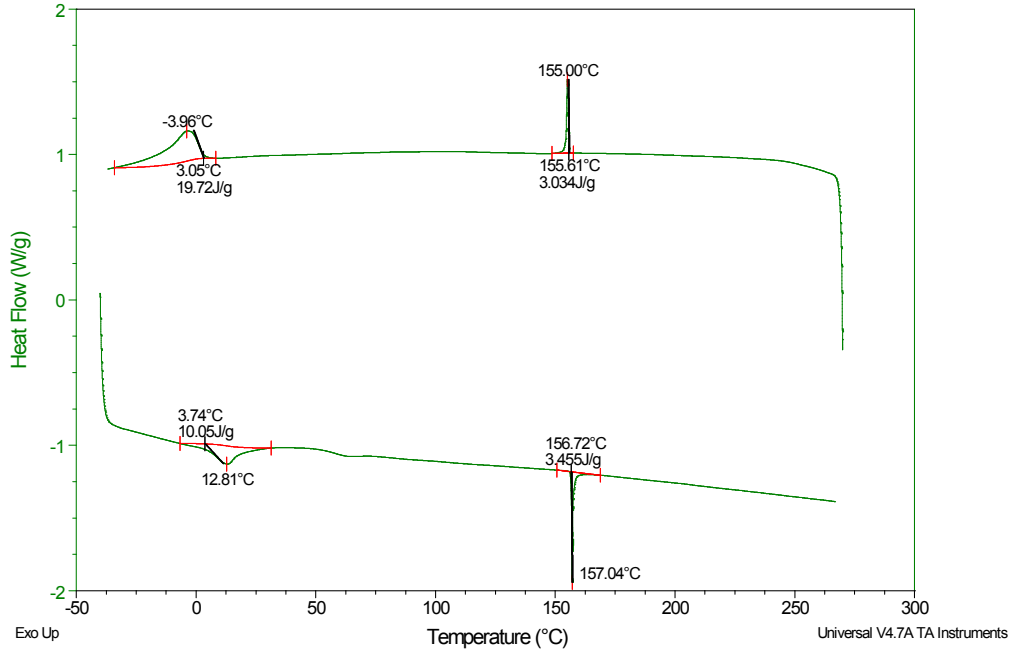


Figure S58. DSC trace (2nd scan) for HBu(12) with a heating and cooling rate of 10 °C min⁻¹.

Sample: jy123-3rd
Size: 1.8000 mg
Method: JY

DSC

File: C:\...Williams Group\JY\jy123-1st.003
Operator: VEW
Run Date: 31-Oct-2014 12:24
Instrument: DSC Q2000 V24.9 Build 121

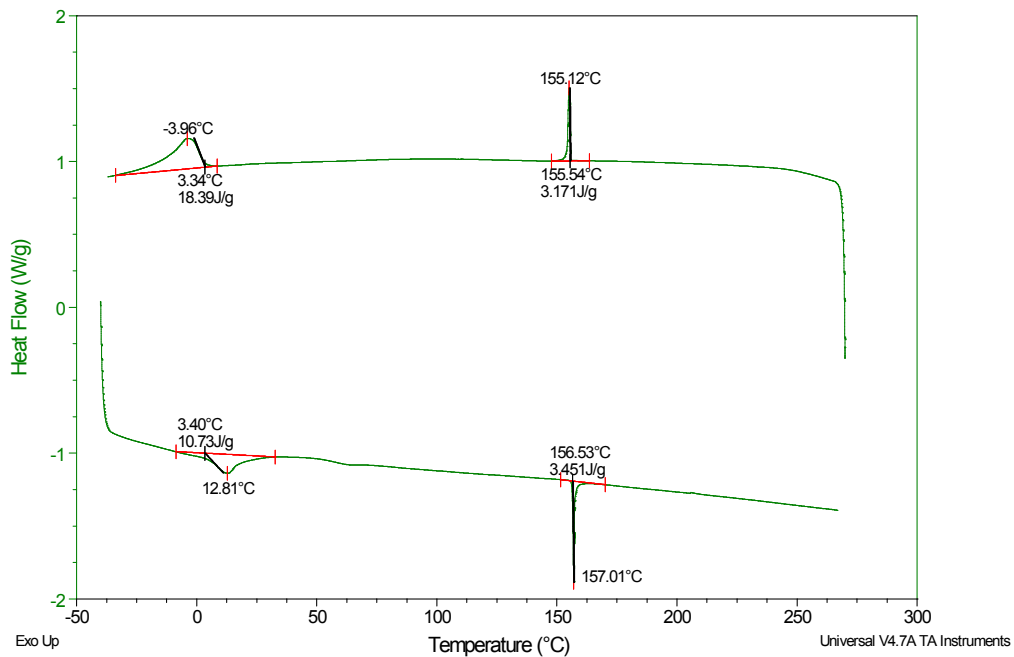


Figure S59. DSC trace (3rd scan) for HBu(12) with a heating and cooling rate of 10 °C min⁻¹.

POM photographs

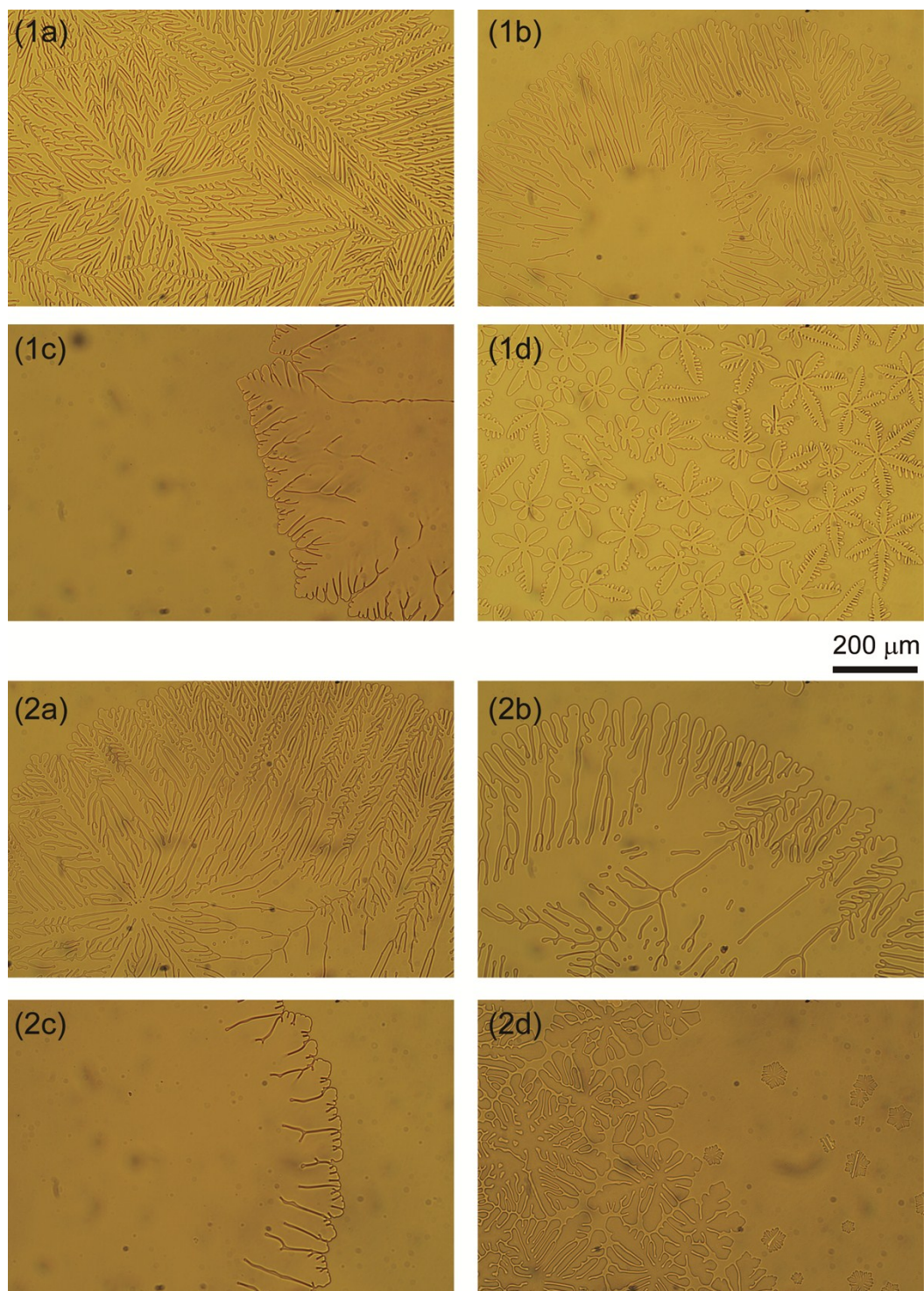


Figure S60. Representative textures observed by optical microscopy for (1a) **dEt(6)**, (1b) **dEt(8)**, (1c) **dEt(10)**, (1d) **dEt(12)**, (2a) **HBu(6)**, (2b) **HBu(8)**, (2c) **HBu(10)**, (2d) **HBu(12)** at 1~6 °C below the clearing temperatures on cooling from the isotropic liquid. All images were taken with polarizers uncrossed.

X-ray diffraction patterns

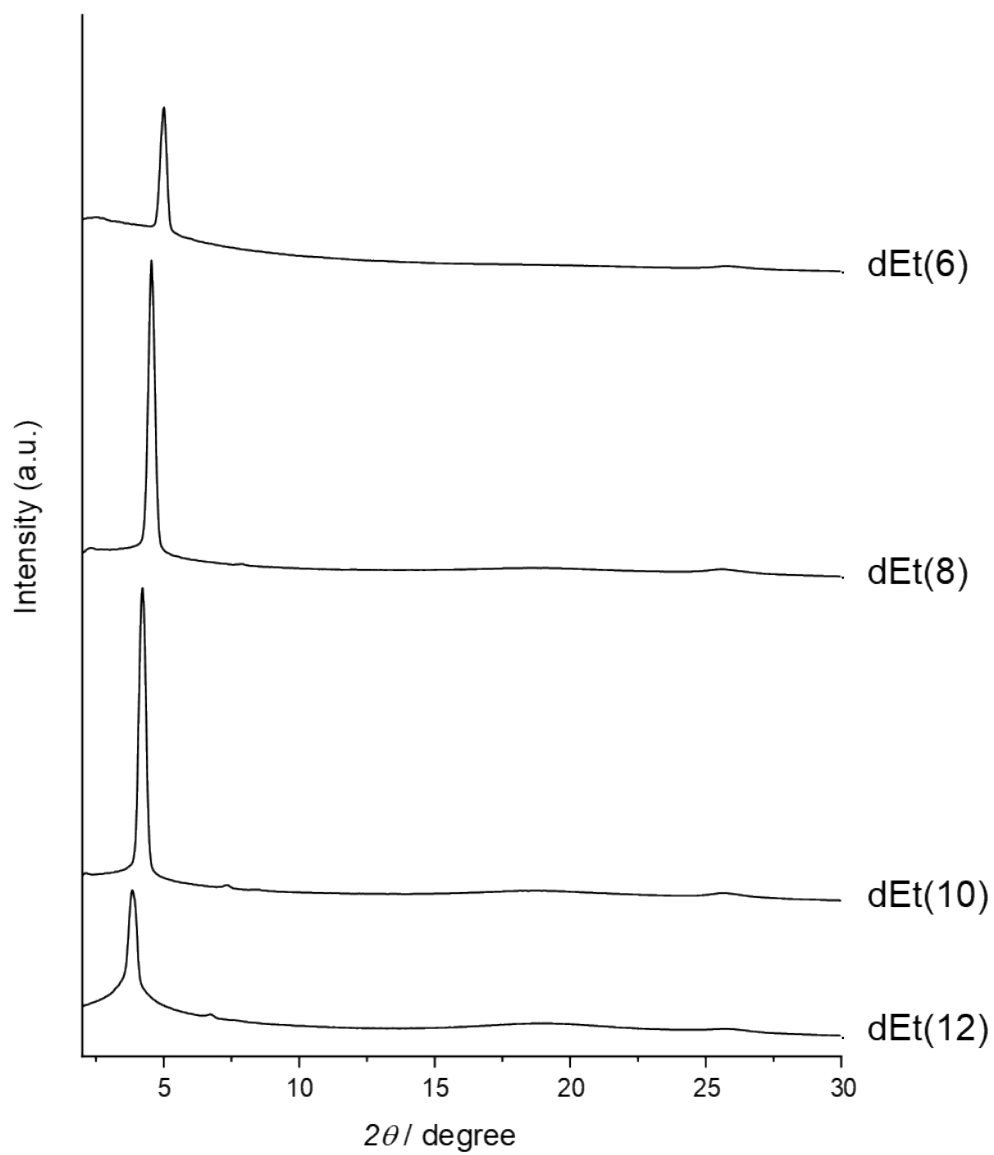


Figure S61. XRD patterns of dibenzophenazines with diethyl amides: **dEt(6)** measured at 135°C, **dEt(8)** at 135°C, **dEt(10)** at 120°C, and **dEt(12)** at 110°C.

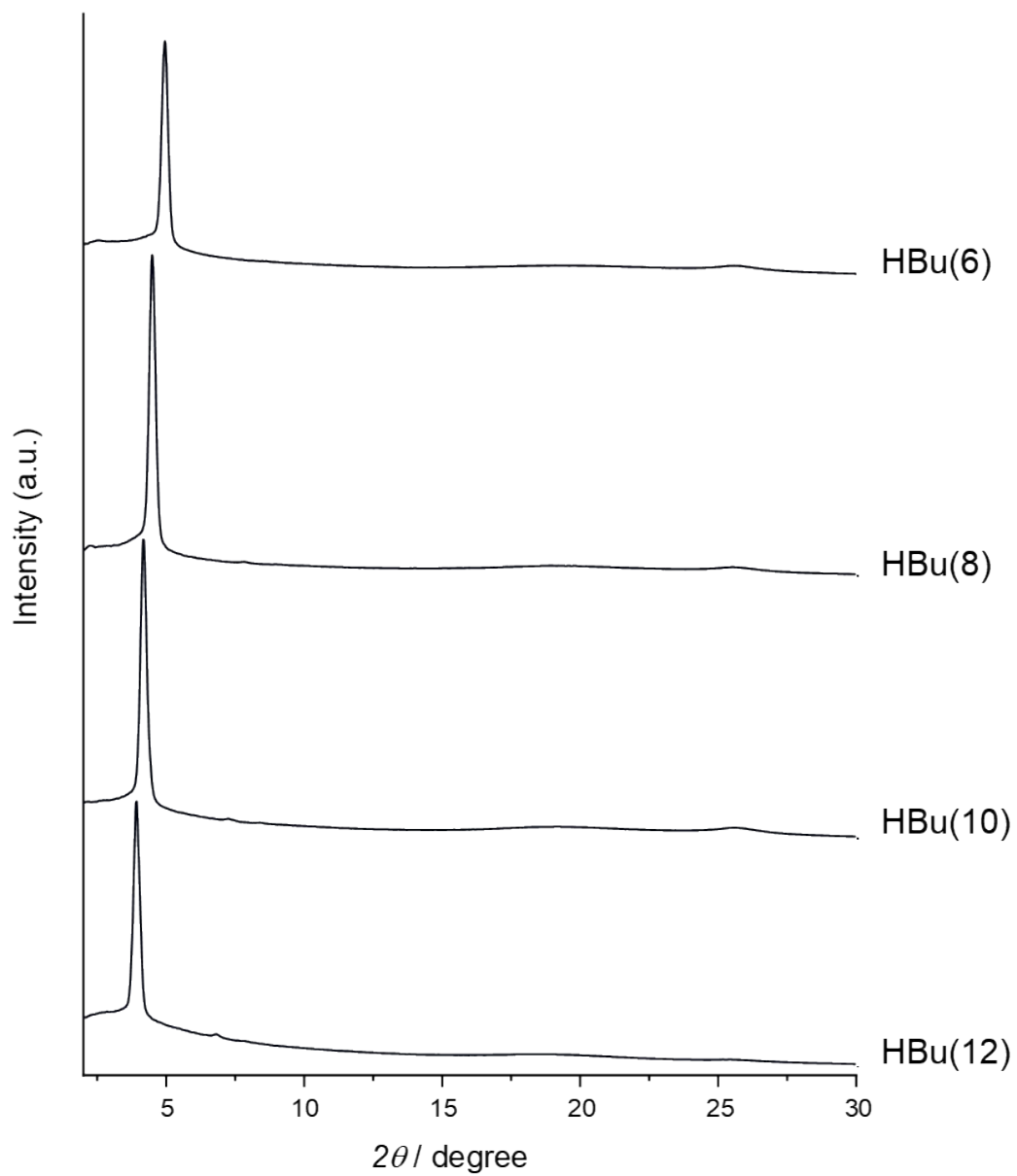


Figure S62. XRD patterns of dibenzophenazines with butyl amides: **HBu(6)** measured at 120°C, **HBu(8)** at 115°C, **HBu(10)** at 115°C, and **HBu(12)** at 150°C.

References

- 1 E. J. Foster, C. Lavigueur, Y.-C. Ke and V. E. Williams, *J. Mater. Chem.*, 2005, **15**, 4062.
- 2 E. J. Foster, R. B. Jones, C. Lavigueur and V. E. Williams, *J. Am. Chem. Soc.*, 2006, **128**, 8569–8574.
- 3 C. Lavigueur, E. J. Foster and V. E. Williams, *J. Appl. Crystallogr.*, 2008, **41**, 214–216.
- 4 C. Lavigueur, E. J. Foster and V. E. Williams, *J. Am. Chem. Soc.*, 2008, **130**, 11791–800.
- 5 G. M. Sheldrick, *Acta Crystallogr. Sect. A Found. Crystallogr.*, 2015, **71**, 3–8.
- 6 G. M. Sheldrick, *Acta Crystallogr. Sect. C Struct. Chem.*, 2015, **71**, 3–8.
- 7 O. V. Dolomanov, L. J. Bourhis, R. J. Gildea, J. A. K. Howard and H. Puschmann, *J. Appl. Crystallogr.*, 2009, **42**, 339–341.